



The Transport of Non-Elliptical Beams

Adam Watts

Fermilab Accelerator Division / External Beams

8 February 2017



Overview Of This Talk

- My Background
- Overview of Fermilab Accelerator Complex
- Particle Accelerators and Beamlines
- Beam Optics Fundamentals
- Beam Measurement
- Nonlinear Magnets and Non-elliptical Beam
- Computed Beam Tomography

My Background

- B.S. in Engineering Physics from University of Illinois (UIUC)
 - Senior thesis: “Spectral Analysis of the French Horn and the Hand-in-Bell Effect”

Conn 8D Open F-Side |Zin| Comparison for Hand Placement
Adam Watts 7/2/09

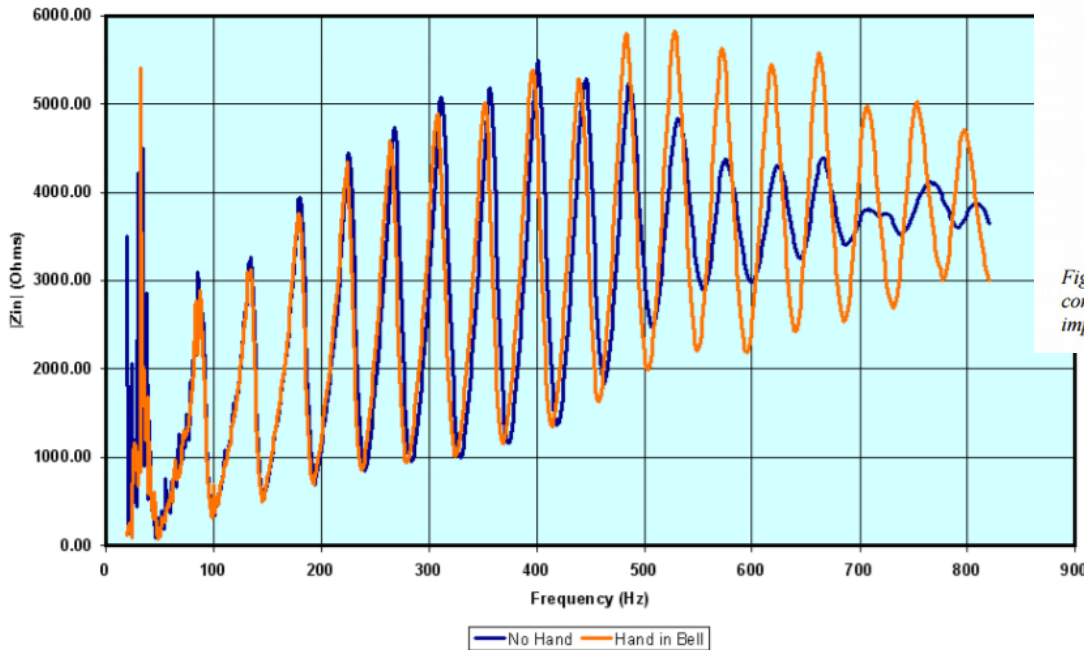


Figure 12: Input impedance of the French Horn as a function of excitation frequency of the air column via the mouthpiece. The comparison is made for no hand in the bell (blue) and normal hand playing position (orange). The addition of the hand has a pronounced effect on higher notes (curve peaks), increasing note stability (peak height) and lowering note pitch (frequency). The first peak is known to be due to 1/f ventilation noise.

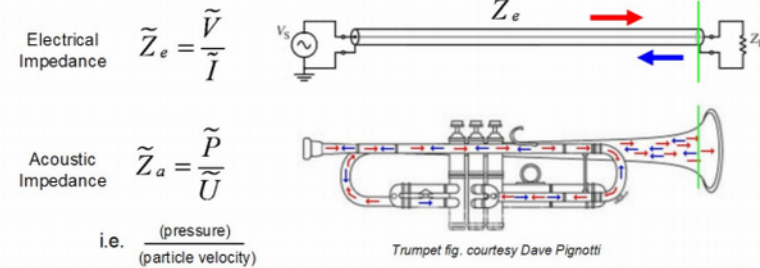


Figure 4: The brass instrument as an analog to the electrical transmission line, with correspondingly defined acoustic impedance to measure wave reflection (blue) at source/load impedance mismatch (green line). Red represents the incident wave or electrical signal.



Figure 1: Typical hand position for playing the French Horn. Slightly cupping the hand closed lowers the pitch.

My Background

- Fermilab Accelerator Operations, Main Control Room Operator 4 years (excellent entry-level position!!)



My Background

- Fermilab Accelerator Operations, Main Control Room Operator 4 years (excellent entry-level position!!)



My Background

- Fermilab External Beamlines, Engineering Physicist, 2.5 years and counting



Currently Machine Coordinator for 2.5 miles of SY beamline, as well as NuMI Coordinator for this month: on-call 24/7, but no shift work!

My Background

- Indiana University M.S. in Beam Physics and Technology
- United States Particle Accelerator School (uspas.fnal.gov)



USPAS Summer 2016, Colorado State University, Physics of Particle Detectors class

Fermilab Accelerators

The Fermilab Accelerator complex consists of a chain of proton particle accelerators and several experimental beamlines. The maximum available beam kinetic energy is 120 GeV, corresponding to protons travelling at 99.997% the speed of light. We deliver beam to a long-baseline neutrino oscillation experimental program (“NuMI”), a short-baseline neutrino oscillation program (“BNB”), a Nuclear Physics experiment and Test Beam Facility** (Switchyard), and soon a Muon experimental program.

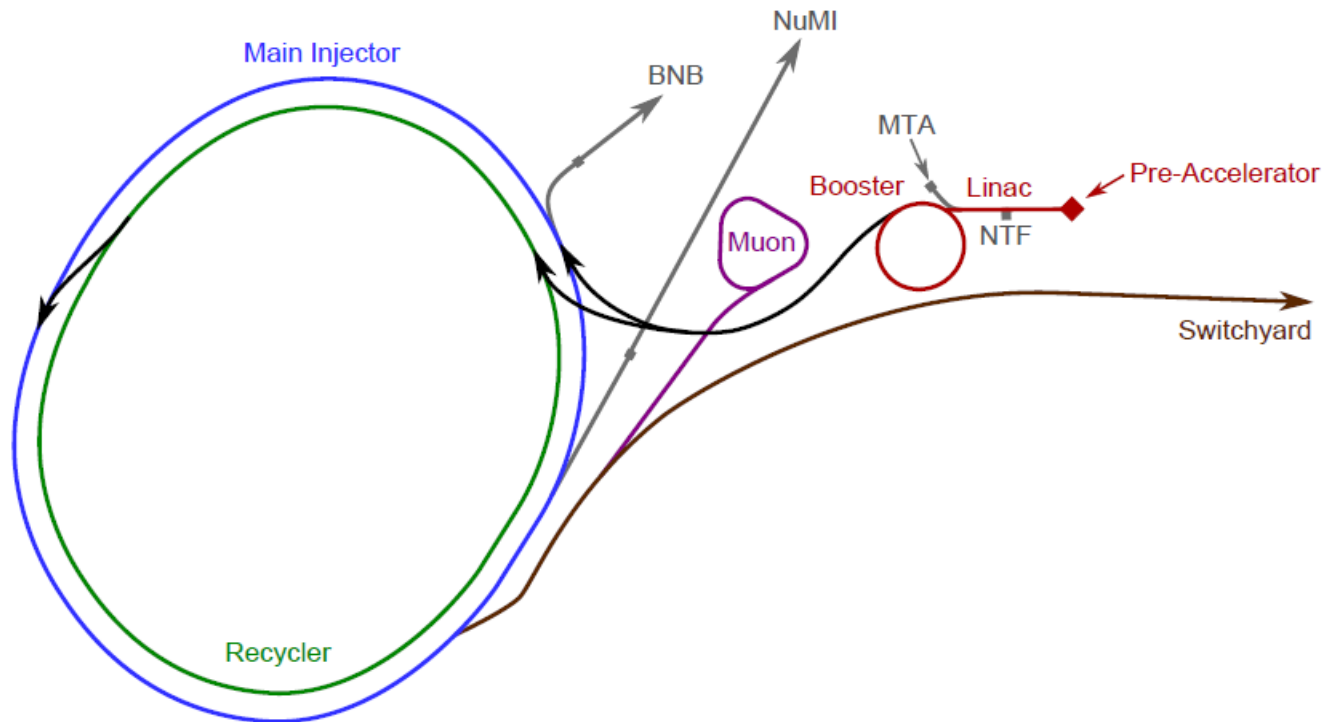


Figure 4.1: Layout of the accelerators at Fermilab

**Run by NCC's own Physics adjunct and Fermilab scientist Mandy Rominsky

Particle Accelerators and Beamlines

Particle accelerators increase the kinetic energy of a group of particles (i.e. “beam”) and direct those particles to an experiment. Electric field “kicks” from high-frequency electromagnetic resonant structures called “RF Cavities” increase particle kinetic energy. Magnets steer and focus the particles.



Figure 1.3: A simple linear accelerator

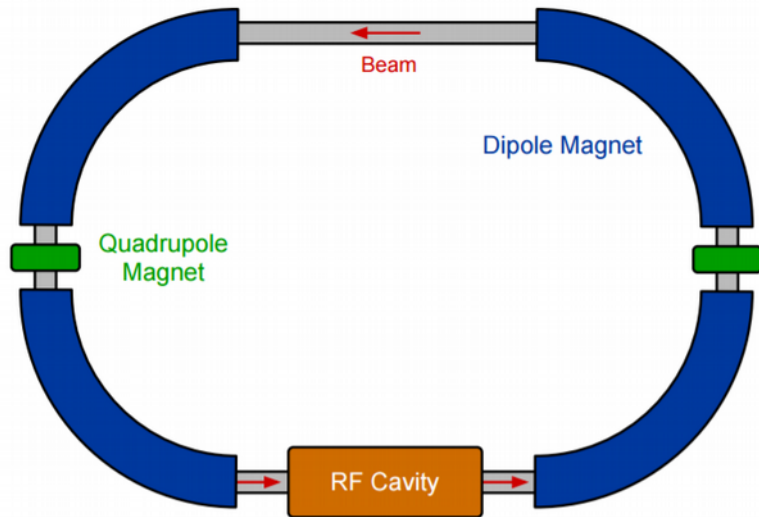


Figure 1.4: A simple synchrotron

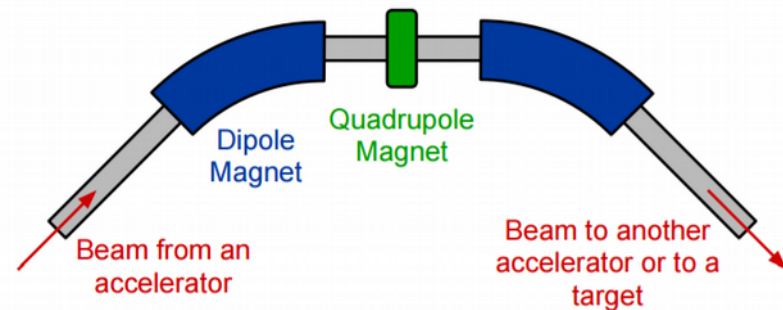
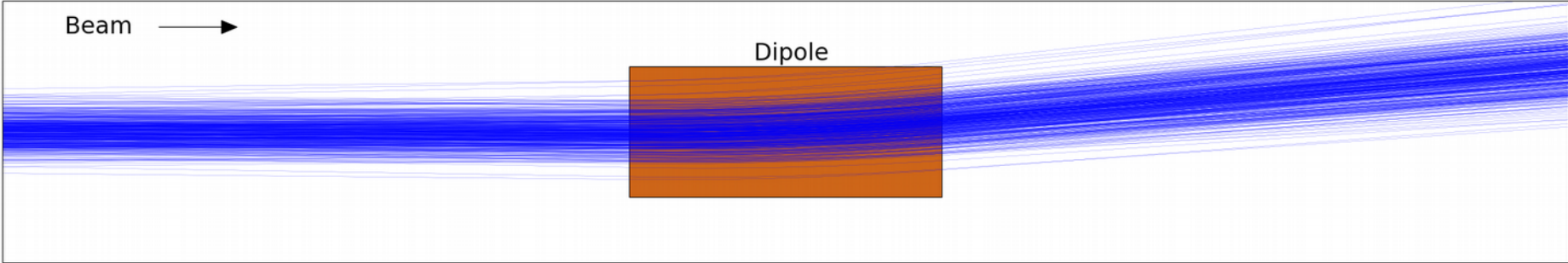
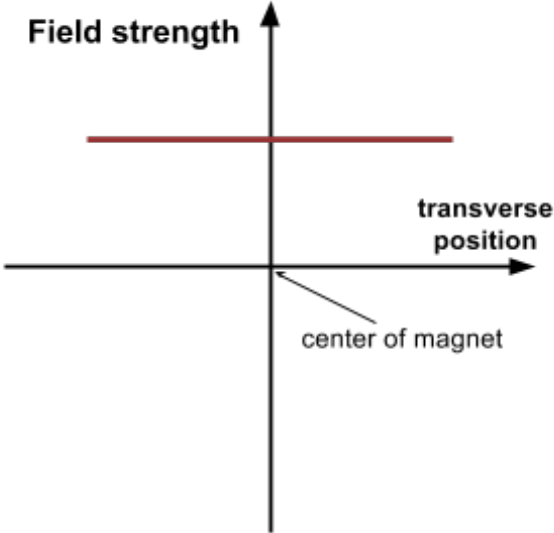
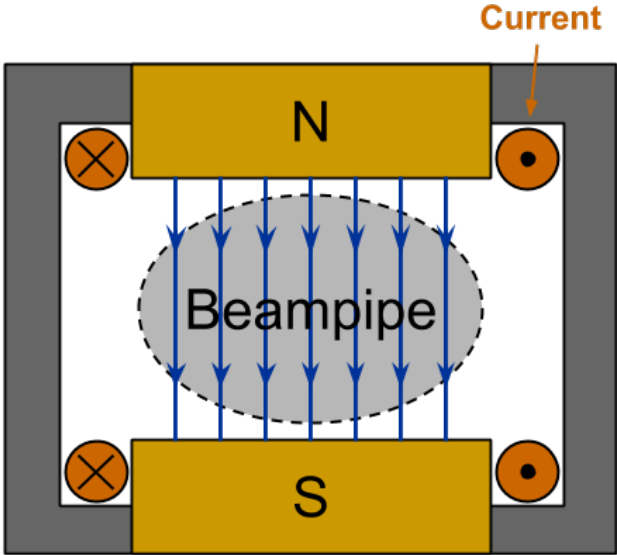


Figure 1.5: A simple beamline

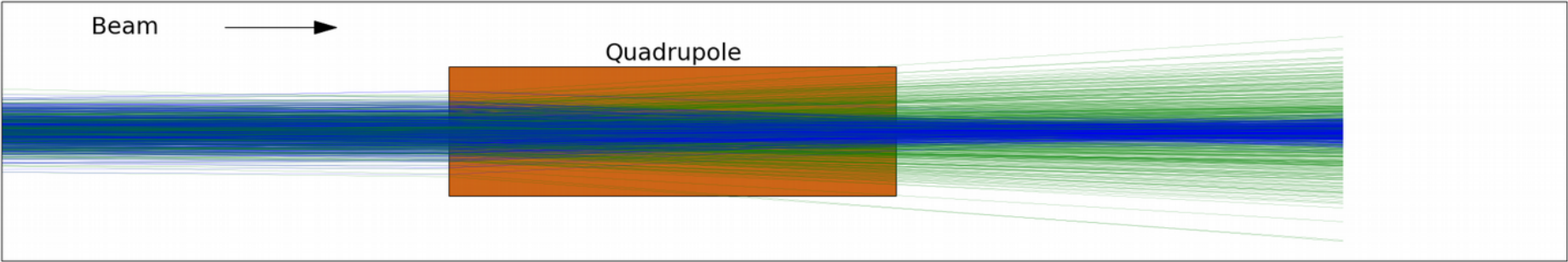
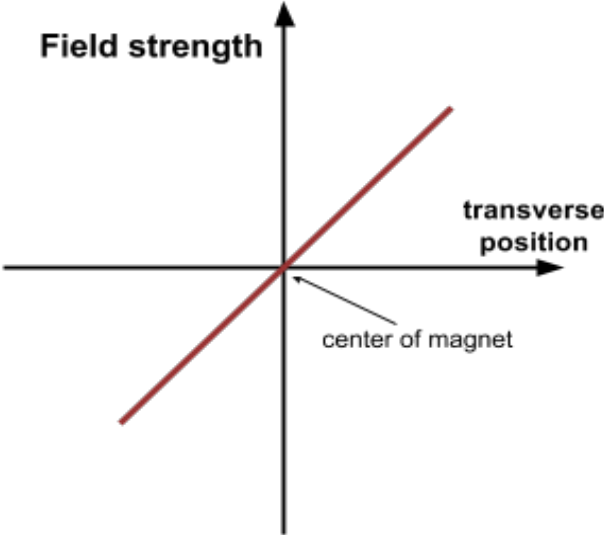
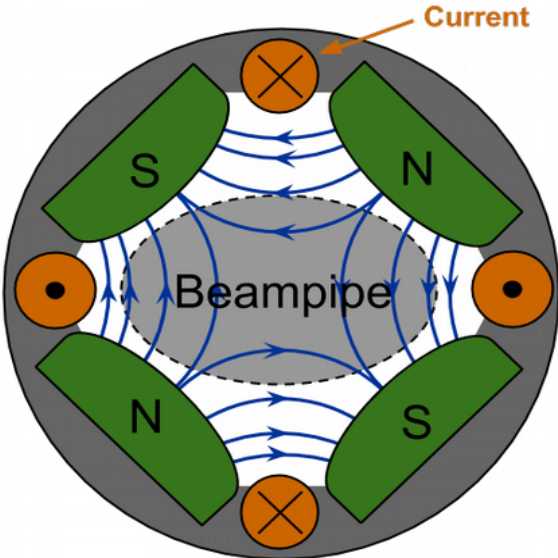
Particle Transport, Dipole Electromagnet

High energy particle beams are typically directed and focused by magnetic fields. Dipole magnets steer the beam trajectory. However, due to non-zero beam divergence (particle angles), beam size increases over distance.



Particle Transport, Quadrupole Electromagnet

To focus the beam, we typically use quadrupole magnets. These provide a linear restoring force toward the center of the magnet, thus acting like a lens; however, a quadrupole always focuses in one plane and de-focuses in the other. (Blue is horizontal beam, green is vertical in bottom diagram)



Single-Particle Transport Theory

Assuming the focal length of the magnetic lens is much longer than the actual magnet (i.e. “thin-lens approximation”), the quadrupole magnet's effect on a single particle's position (x and y) and angle (x' and y') is the following:

$$\begin{pmatrix} x_1 \\ x'_1 \end{pmatrix} = \begin{pmatrix} 1 & 0 \\ -\frac{1}{f} & 1 \end{pmatrix} \begin{pmatrix} x_0 \\ x'_0 \end{pmatrix} \qquad \begin{pmatrix} y_1 \\ y'_1 \end{pmatrix} = \begin{pmatrix} 1 & 0 \\ \frac{1}{f} & 1 \end{pmatrix} \begin{pmatrix} y_0 \\ y'_0 \end{pmatrix}$$

The focal length depends on the integrated field strength gradient (B') over the magnet's length (L), as well as the particle's momentum and charge. Higher-momentum particles are “harder” to deflect with magnetic fields; we parametrize this as the “magnetic rigidity”, ($B\rho$).

$$\frac{1}{f} = \frac{B'L}{(B\rho)} \qquad (B\rho) = \frac{p}{q}$$

As a side note, the angular deflection from a thin dipole is similarly computed by:

$$\Delta\theta = \frac{BL}{(B\rho)}$$

Particle Transport, Quadrupole Doublet

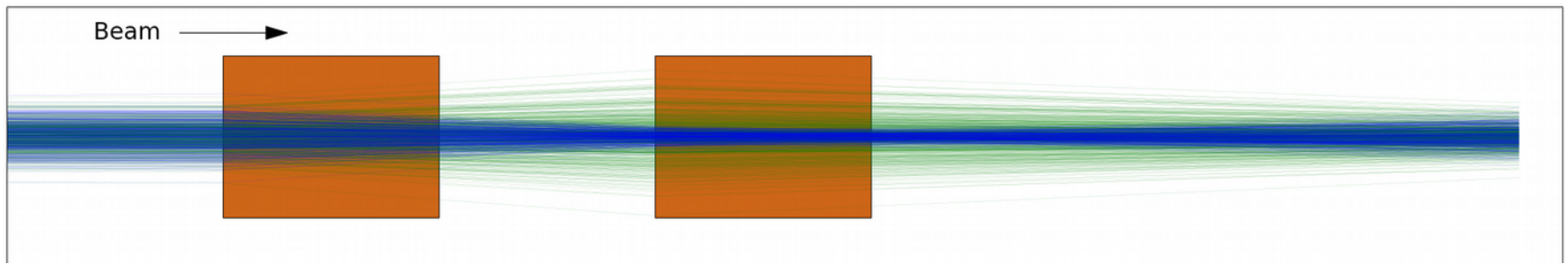
To compute the effect of multiple beamline elements on a single particle vector, simply multiply the transfer matrices together *in the order the beam sees them*; remember, matrix multiplication is not commutative, so the order matters. We can lump all the beamline elements into a single “transfer matrix”, here denoted by “M”.

$$\begin{pmatrix} x_1 \\ x'_1 \end{pmatrix} = M \begin{pmatrix} x_0 \\ x'_0 \end{pmatrix}$$

For example, let's look at a quadrupole doublet, which is two quadrupole magnets of opposite polarity separated by a small drift (no-magnet space) of length d .

$$M = \begin{pmatrix} 1 & 0 \\ -\frac{1}{f} & 1 \end{pmatrix} \begin{pmatrix} 1 & d \\ 0 & 1 \end{pmatrix} \begin{pmatrix} 1 & 0 \\ \frac{1}{f} & 1 \end{pmatrix} = \begin{pmatrix} 1 + \frac{d}{f} & d \\ -\frac{d}{f^2} & 1 - \frac{d}{f} \end{pmatrix}$$

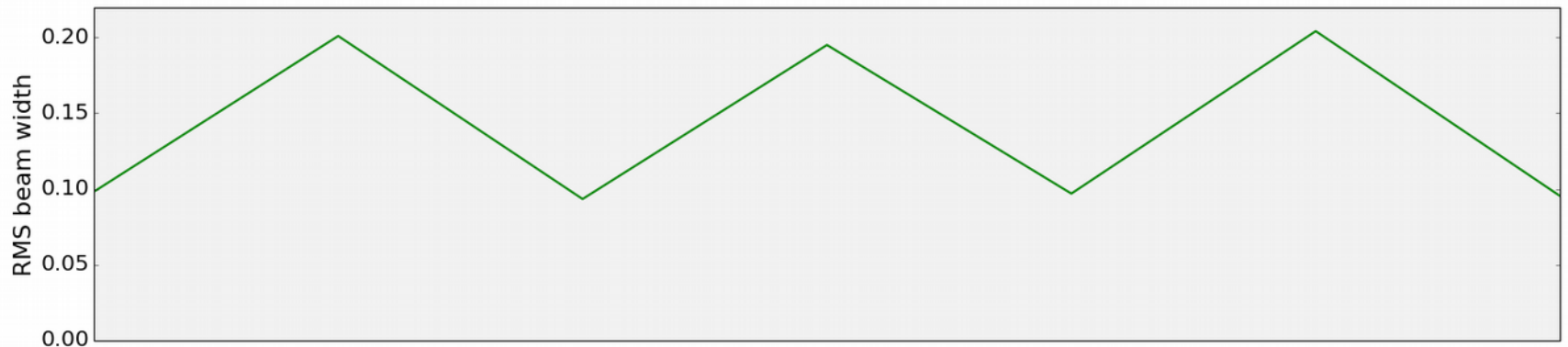
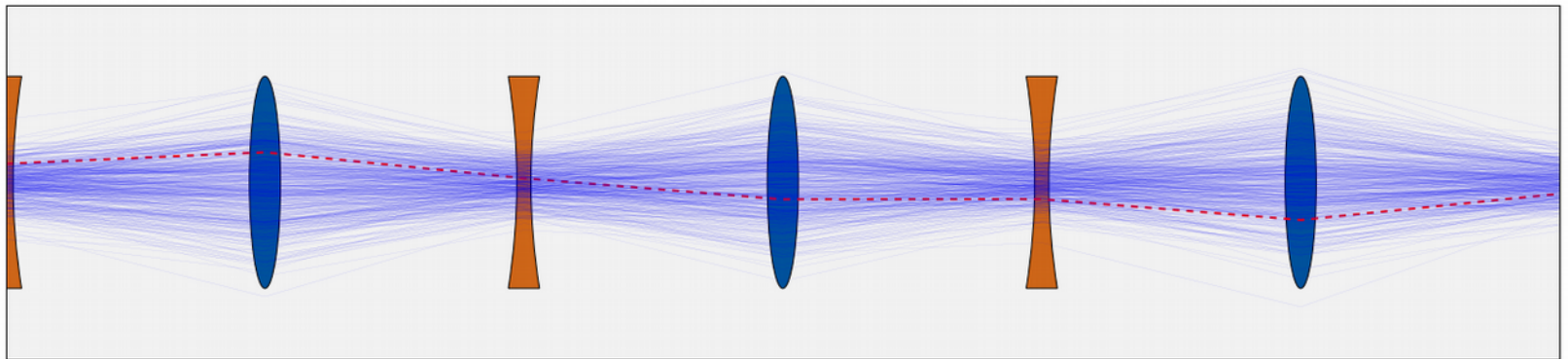
We now have net focusing in both planes with equivalent focal length: $f^* = \frac{f^2}{d}$



Beam Transport, Strong Focusing

For long-distance beam transport, or to design a stable circular accelerator, it is advantageous to use “Strong Focusing”, or “Alternating Gradient Focusing”. This is a periodic arrangement of quadrupoles that alternate polarity, like stringing doublets together indefinitely. This technique allows for stable transport of beam over arbitrarily-long distances without net increase in the beam size in either plane. Beam size oscillations are known as “betatron oscillations”.

- Christofilos, N. C. (1950). "Focusing System for Ions and Electrons". US Patent No. 2,736,799.
- Courant, E. D.; Snyder, H. S. (Jan 1958). "Theory of the alternating-gradient synchrotron" (PDF). *Annals of Physics*. 3 (1): 1–48. Bibcode:2000AnPhy.281..360C. doi:10.1006/aphy.2000.6012.



Multiple-particle Transport Theory

Now we develop the mathematics for describing the group of particles. Typical beam intensities at Fermilab are ~trillions of particles, which are too many to keep track of with single-particle theory. Instead, we focus on the statistical distributions of the particles, i.e. first and second moments.

First moments $\langle x \rangle$ and $\langle x' \rangle$ are average of all the particle positions and angles, and propagate the same as the single particle:

$$\begin{pmatrix} \langle x_1 \rangle \\ \langle x'_1 \rangle \end{pmatrix} = M \begin{pmatrix} \langle x_0 \rangle \\ \langle x'_0 \rangle \end{pmatrix}$$

The second moments $\langle x^2 \rangle$, $\langle x'^2 \rangle$, and $\langle xx' \rangle$ are the variances (standard deviation squared) in position and angle, and the average correlation between position and angle. The second moments propagate as follows:

$$\Sigma_x = \begin{pmatrix} \langle x^2 \rangle & \langle xx' \rangle \\ \langle xx' \rangle & \langle x'^2 \rangle \end{pmatrix} \quad \Sigma_1 = M \Sigma_0 M^T$$

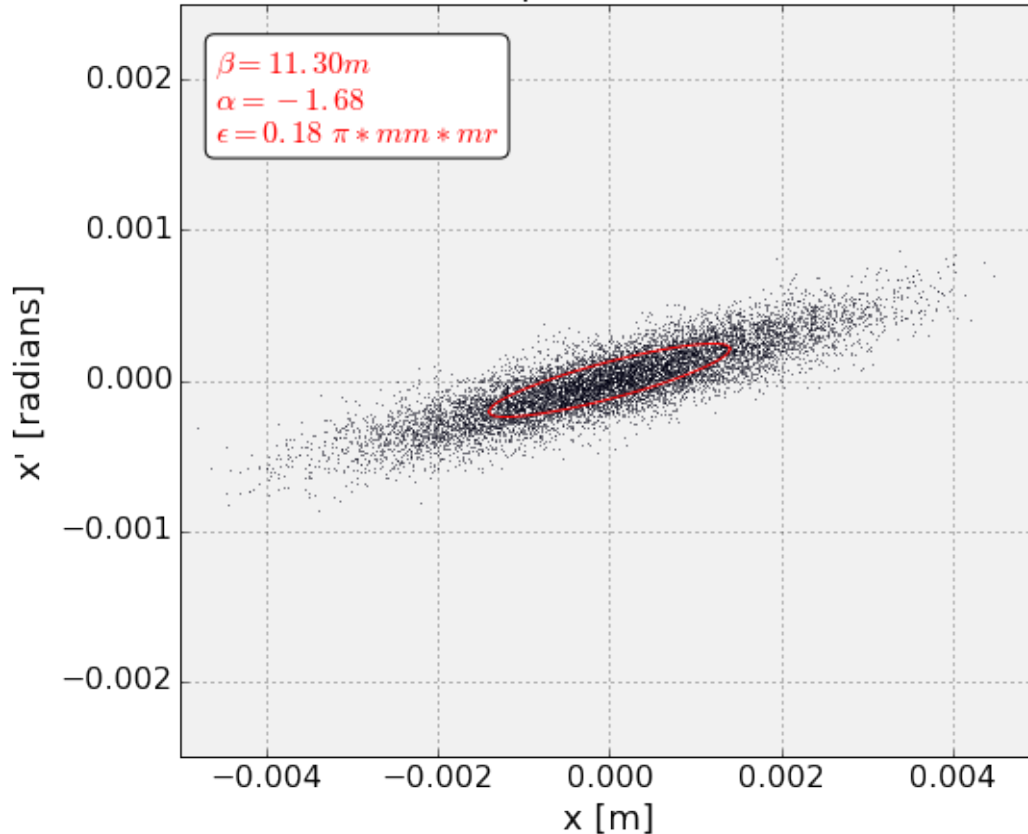
Typically, particle angles are very small and difficult to measure. Usually, we are only able to measure the transverse beam profile at a single point using a profile monitor (like a screen). Thus we can fit a Gaussian curve and compute:

$$\sigma_x = \sqrt{\langle x^2 \rangle}$$

Phase Space and Courant-Snyder parametrization

A different way to think about oscillating systems is to use phase space, i.e. plot each particle's position on one axis and angle on the other*. Passing through FODO beamline corresponds to rotation in phase space, and the area of the effective ellipse is invariant. (Note that “s” is the beam path variable.)

Phase Space Distribution



Equation of ellipse:

$$\epsilon = \gamma x^2 + 2\alpha x x' + \beta x'^2$$

where $\alpha = -\frac{\partial\beta}{\partial s}$ and $\gamma = \frac{1 + \alpha^2}{\beta}$

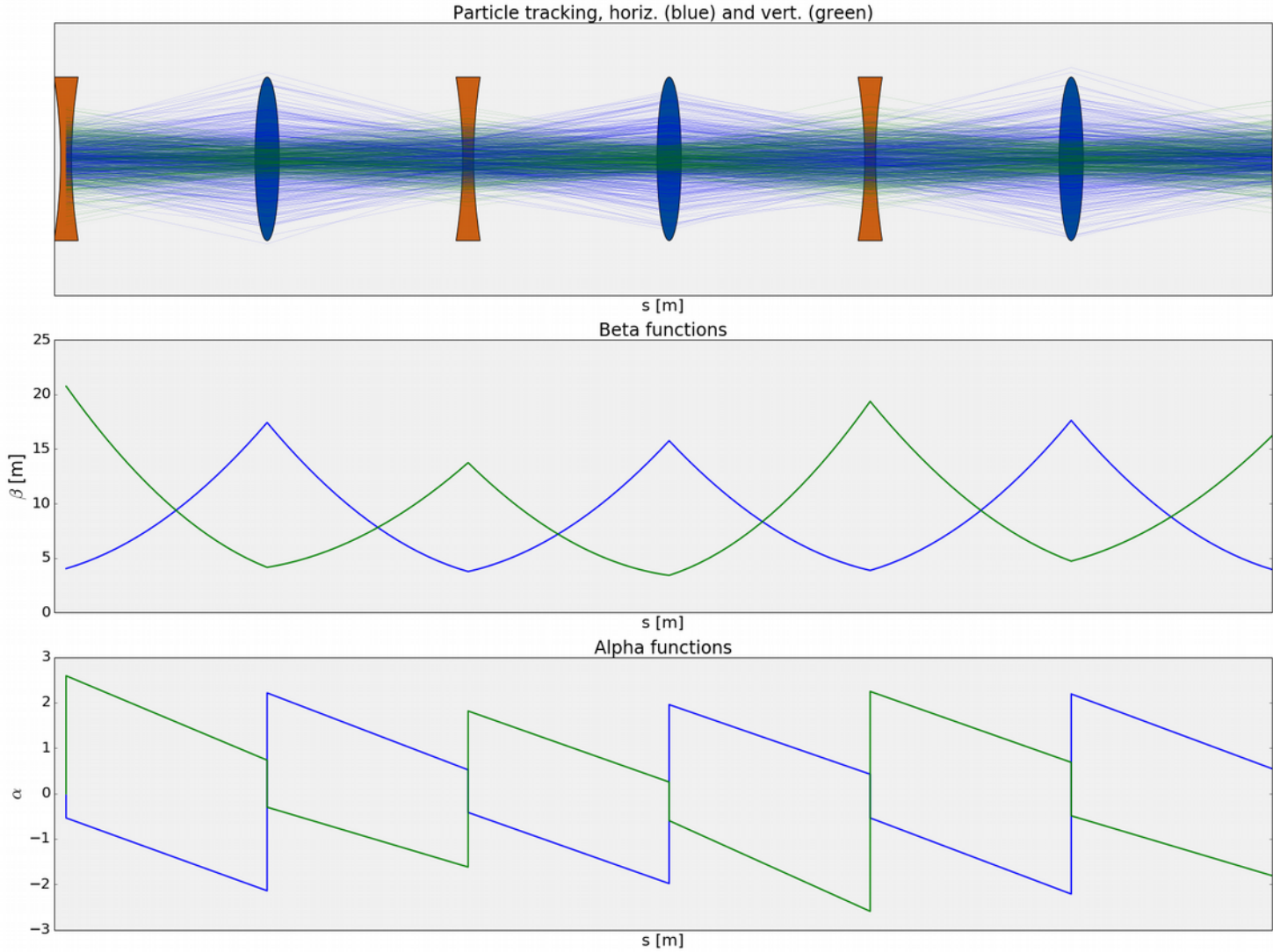
These Courant-Snyder parameters are related to the beam second moments:

$$\epsilon = \sqrt{\langle x^2 \rangle \langle x'^2 \rangle - \langle x x' \rangle^2}$$

$$\alpha = \frac{-\langle x x' \rangle}{\epsilon} \quad \beta = \frac{\langle x^2 \rangle}{\epsilon}$$

*Technically, to satisfy Hamilton's equations of motion, you should use the position and momentum for each plane as the phase space pairs. This requires a Relativistic correction: $p_x = m_0 c (\beta \gamma) x'$

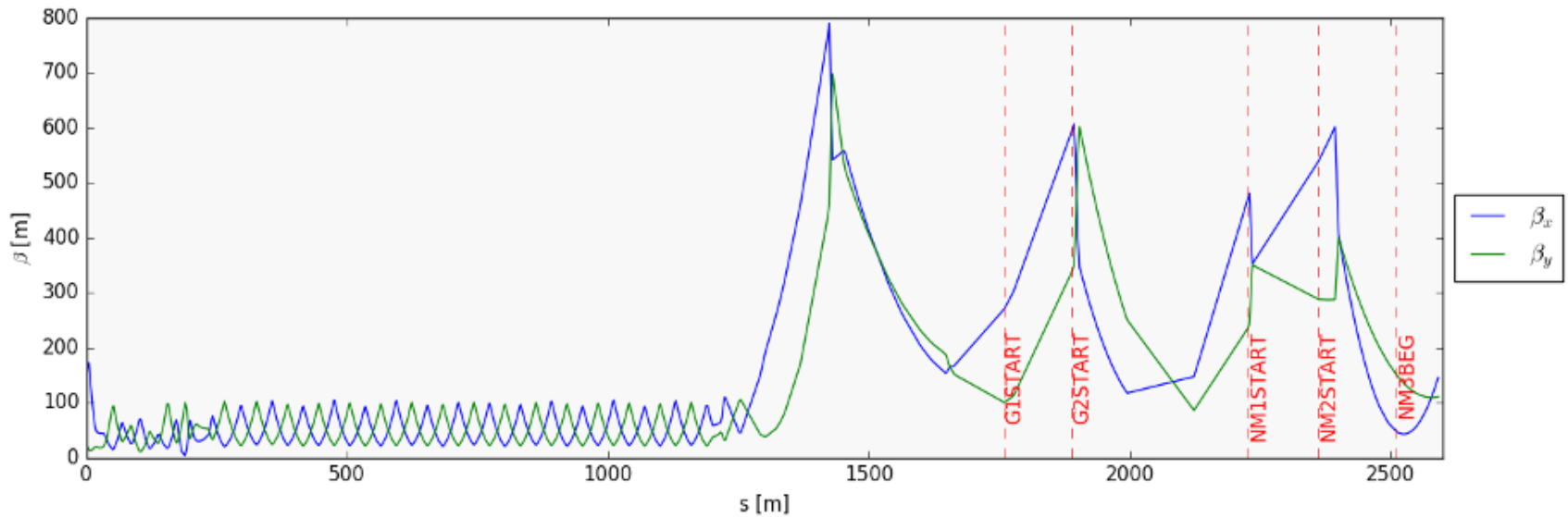
Courant-Snyder parametrization in beamlines



Courant-Snyder parametrization in beamlines

Critical point: The Courant-Snyder parameters form the initial conditions into any beamline simulation**. Thus in order to simulate our beamlines correctly, we must know the initial Courant-Snyder parameters that go into the beamline. Therefore we need methods of actually measuring the Courant-Snyder parameters using beam instrumentation.

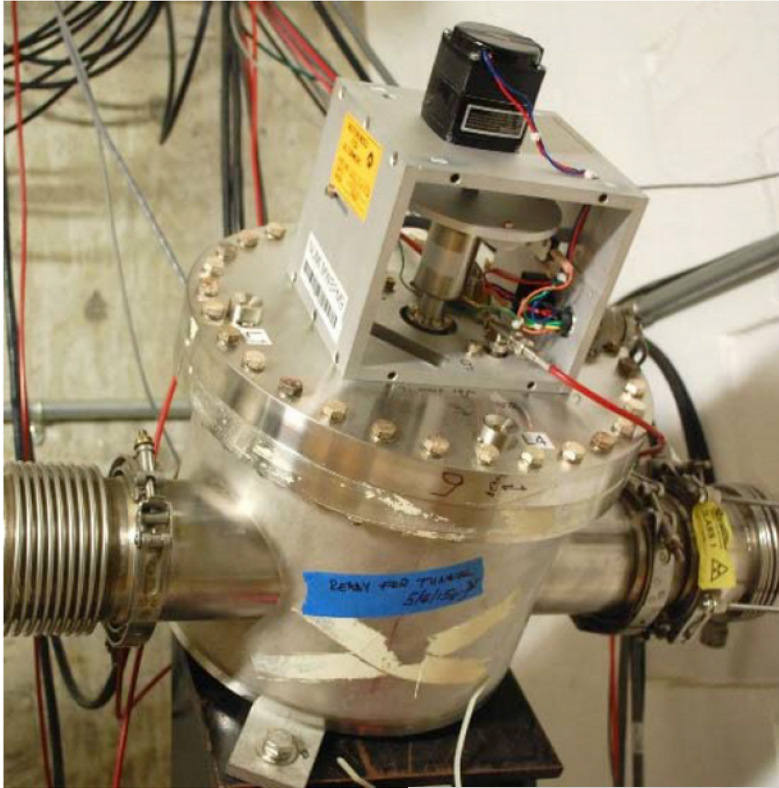
MI52 Lambertson to SeaQuest target



**However, in a circular machine, the Courant-Snyder parameters are uniquely-determined by the magnetic fields; any beam you put in will eventually smear and fill out the ellipse dictated by the magnets.

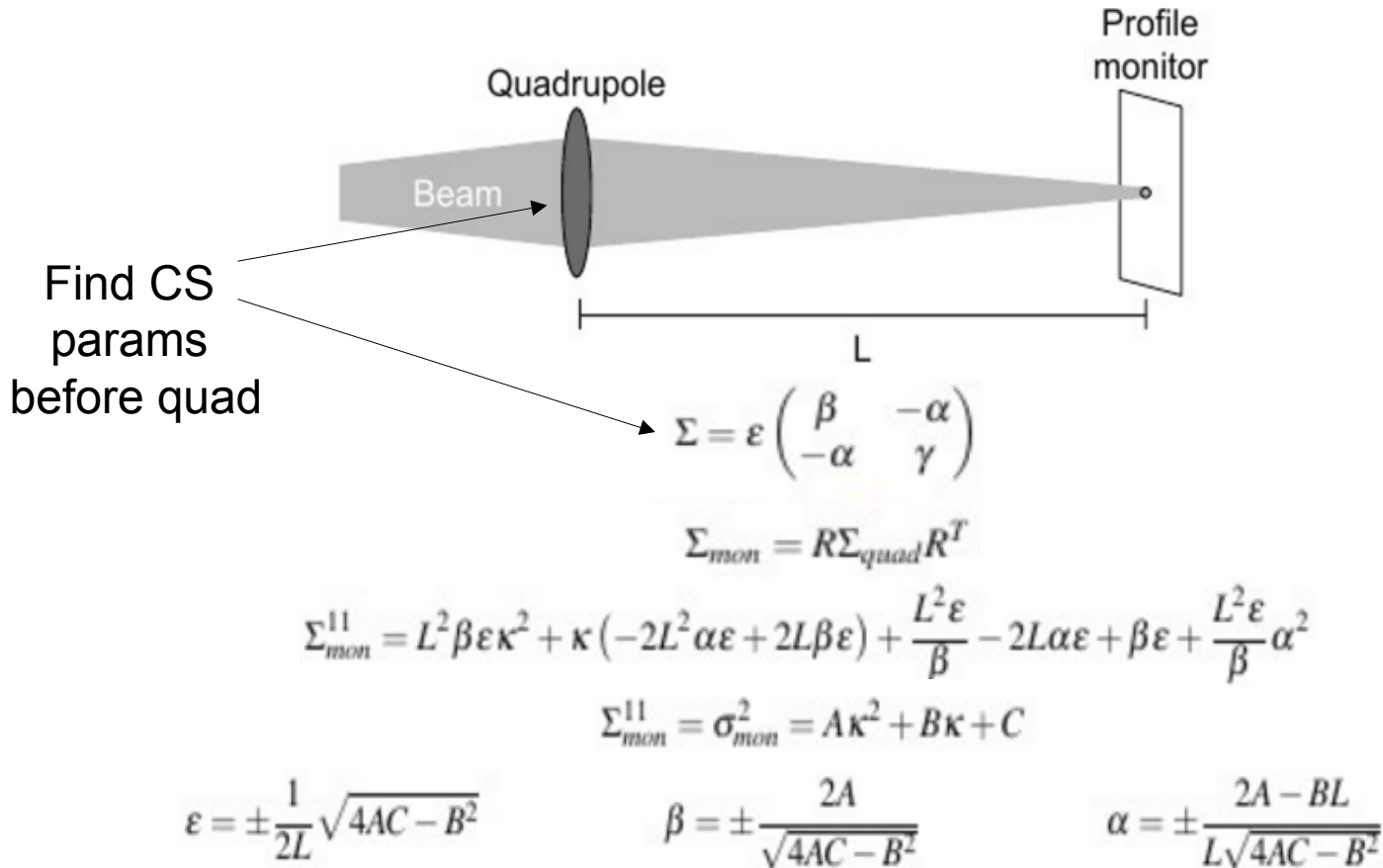
Multiwire Profile Monitors

Most common in Switchyard is the SEM (Secondary Emission Monitor) Multiwire detector. Can be moved in and out of the beam as needed, and provides profile resolution limited by number of wires.



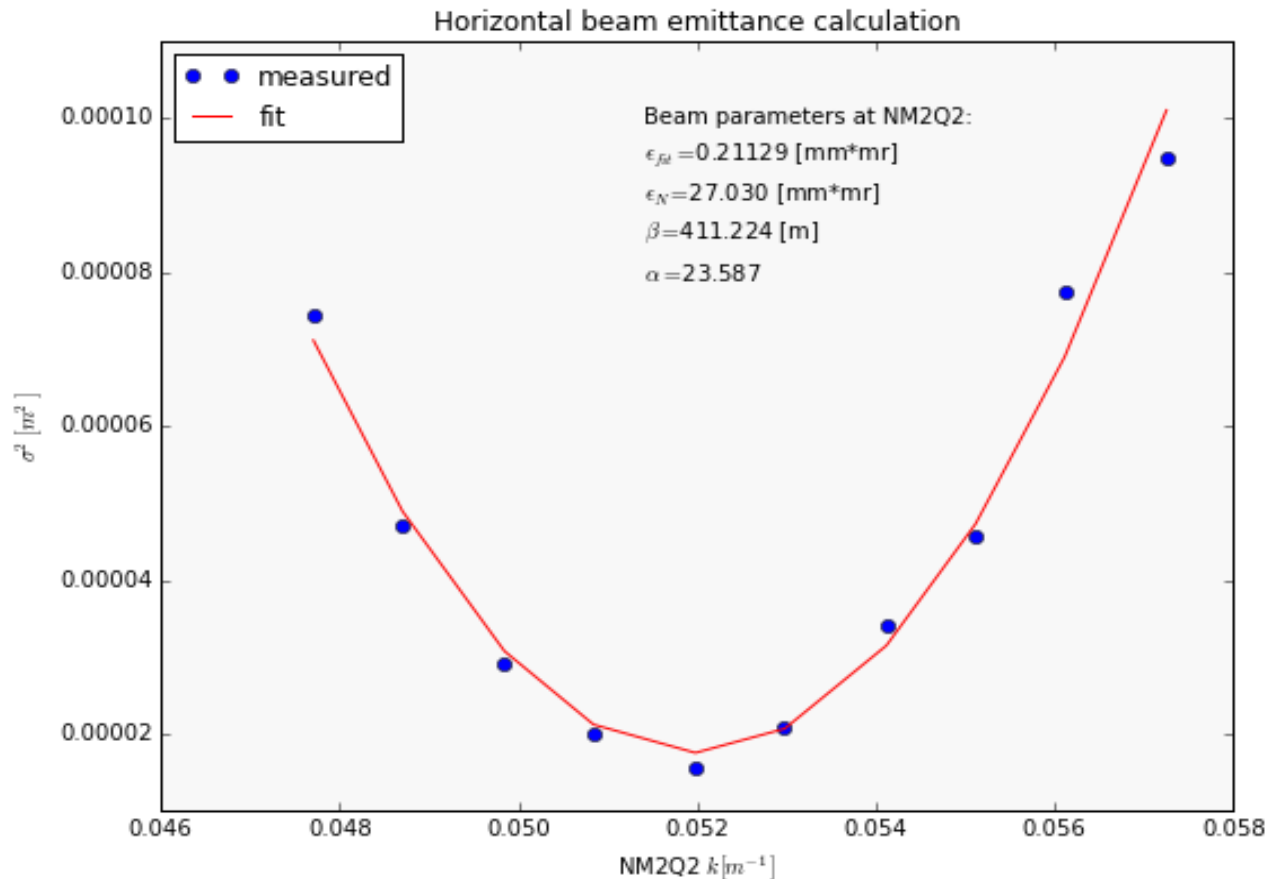
Single-Profile Emittance Measurement

Vary the current in a single quadrupole and measure the beam size for each current setting. If you know the transfer function for the magnet (relationship between current and field strength), and the distance between the magnet and the profile monitor, you can compute the CS parameters for the beam just before the magnet.



Single-Profile Emittance Measurement

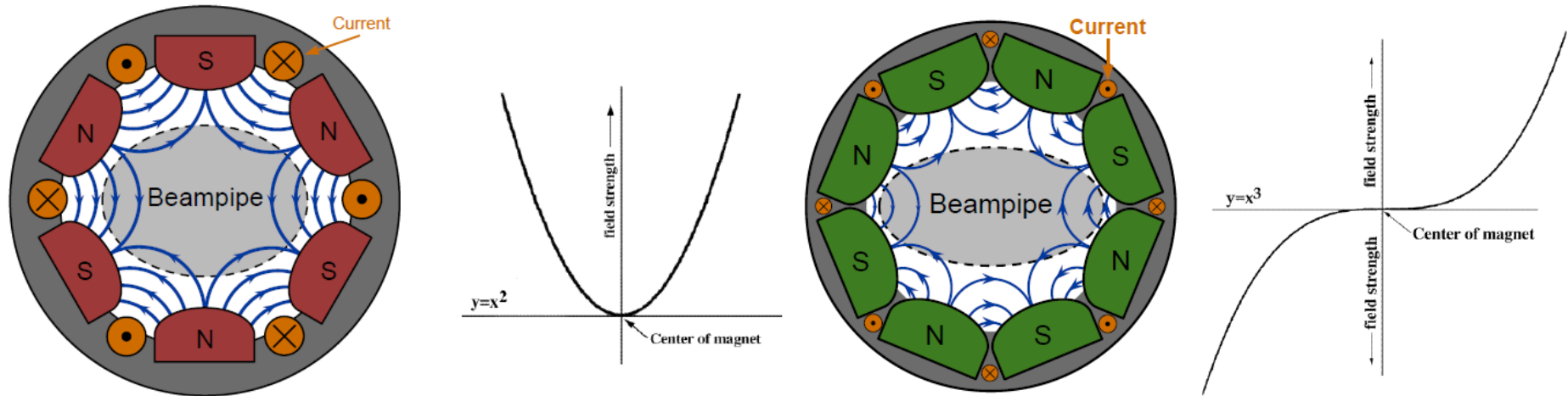
Vary the current in a single quadrupole and measure the beam size for each current setting. If you know the transfer function for the magnet (relationship between current and field strength), and the distance between the magnet and the profile monitor, you can compute the CS parameters for the beam just before the magnet.



Non-linear Magnetic Fields

Magnetic fields are not always linear with transverse displacement, as they are with the dipole (linear, slope zero), and quadrupole. Higher-order magnets such as the Sextupole and Octupole have a non-linear field dependence on the transverse particle position.

These magnets are used for more advanced beam manipulation. However, all magnets have small non-zero higher-order terms that cause non-linear effects (manufacturing or alignment errors, etc.) Sometimes these effects are not so small (MI quadrupoles, for example)!

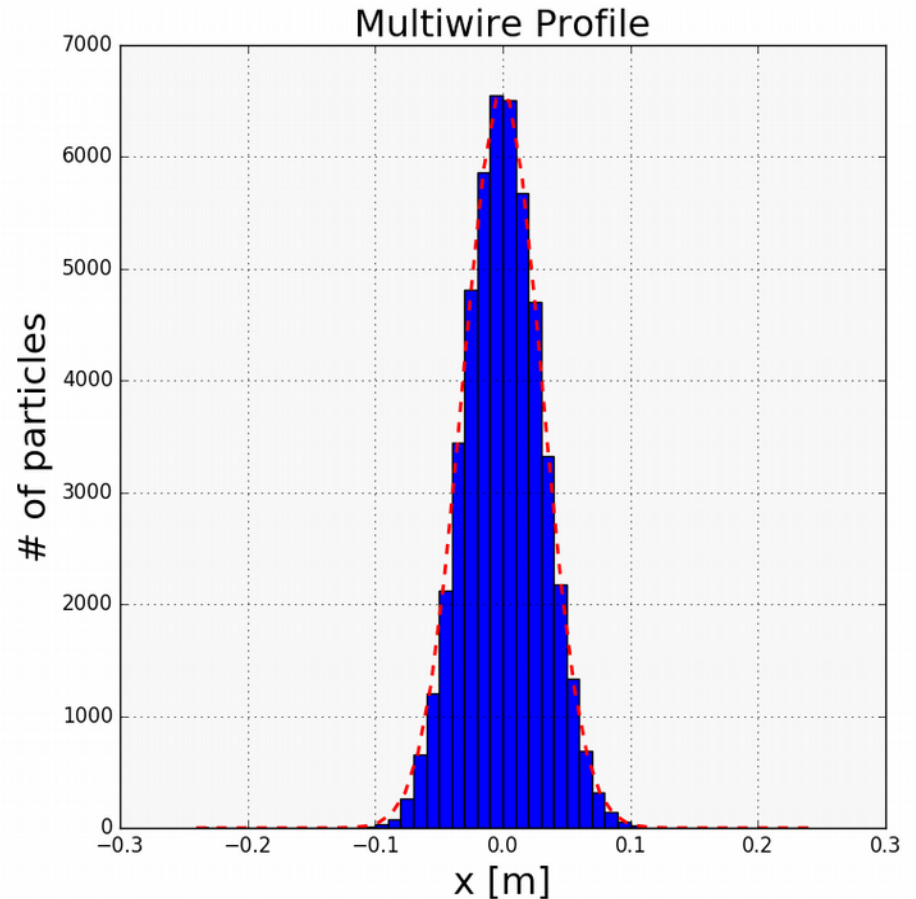
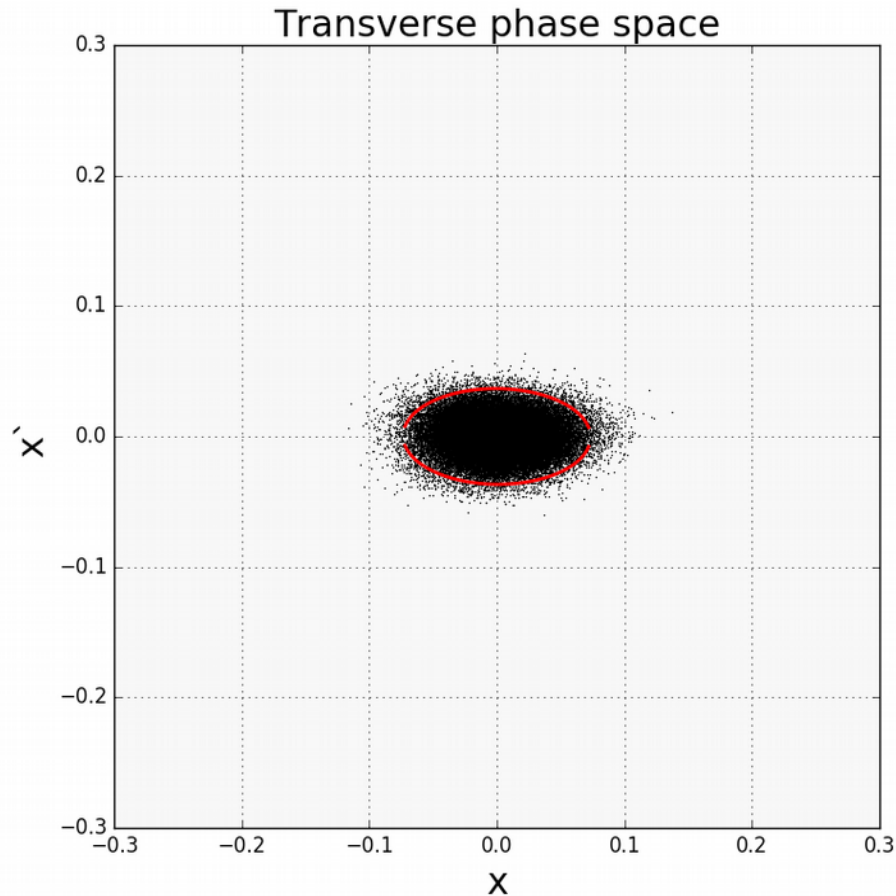


Magnets can be characterized by Taylor Series expansion to describe “accidental” non-linear higher-order effects on the beam due to imperfections.

$$H(x) = \sum_{n=0}^{\infty} a_n x^n = a_0 + a_1 x + a_2 x^2 + \dots$$

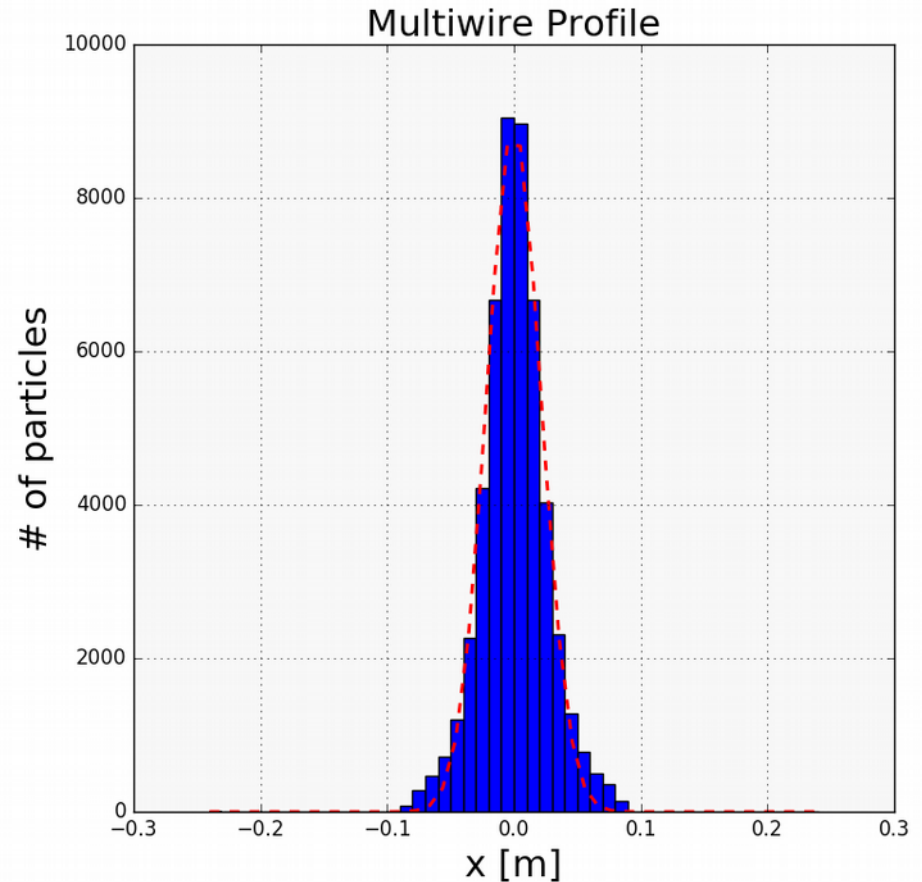
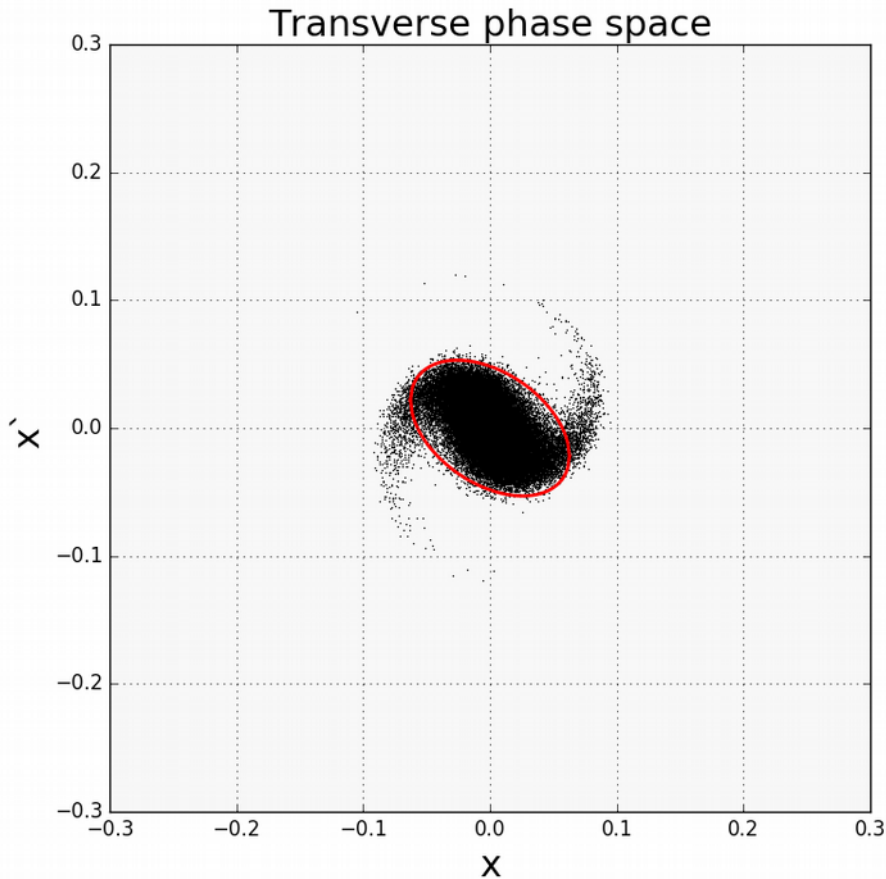
Effect of Non-Linear Fields on Beam

Non-linear fields interact differently with particles on the outside of the ellipse than those toward the core. Thus the fringe particles will rotate at a different rate compared to the core, causing “filamentation”. The beam is no longer elliptical, and requires higher moments to describe. Profiles no longer fit Gaussian distributions as well.



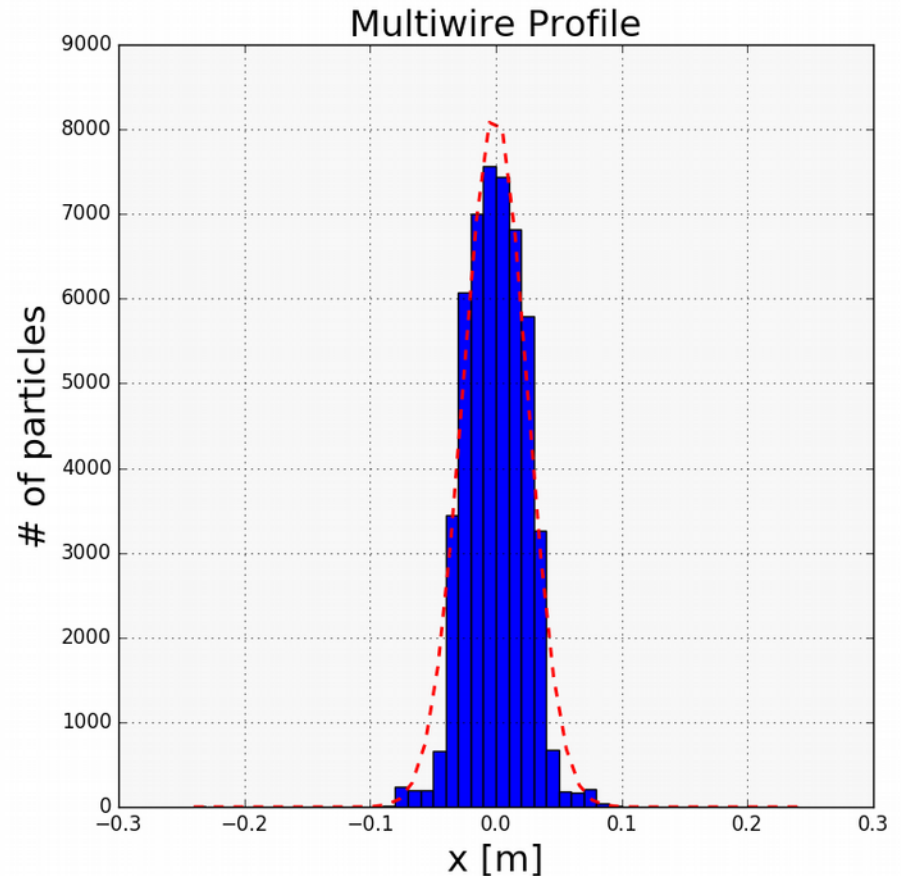
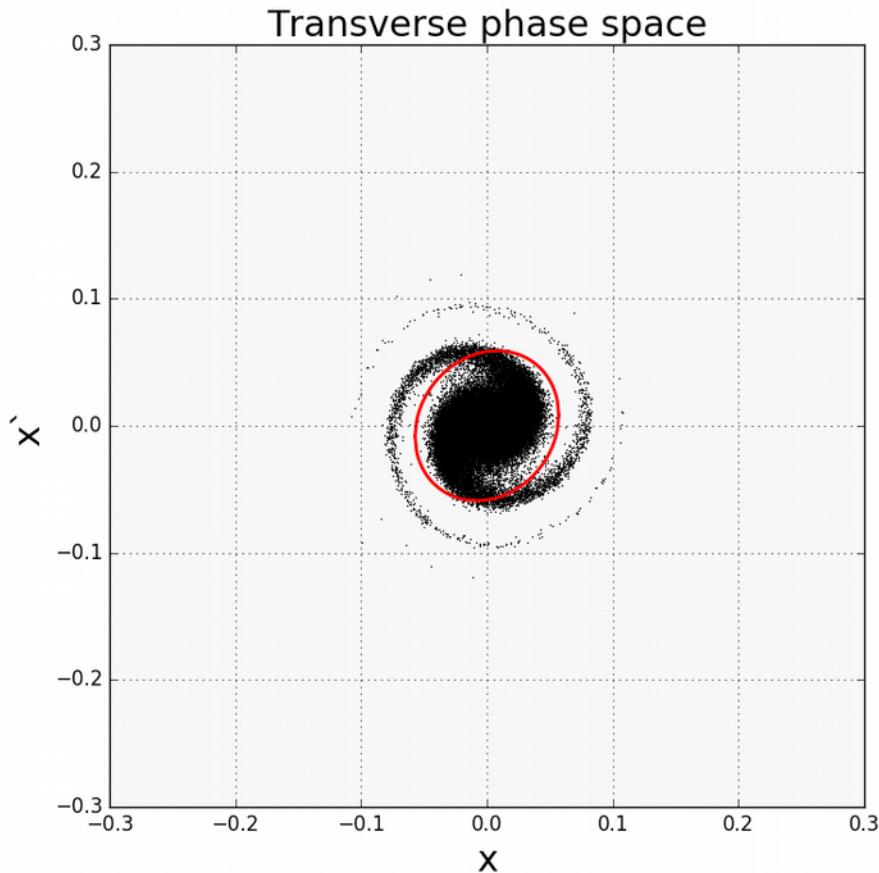
Effect of Non-Linear Fields on Beam

Non-linear fields interact differently with particles on the outside of the ellipse than those toward the core. Thus the fringe particles will rotate at a different rate compared to the core, causing “filamentation”. The beam is no longer elliptical, and requires higher moments to describe. Profiles no longer fit Gaussian distributions as well.



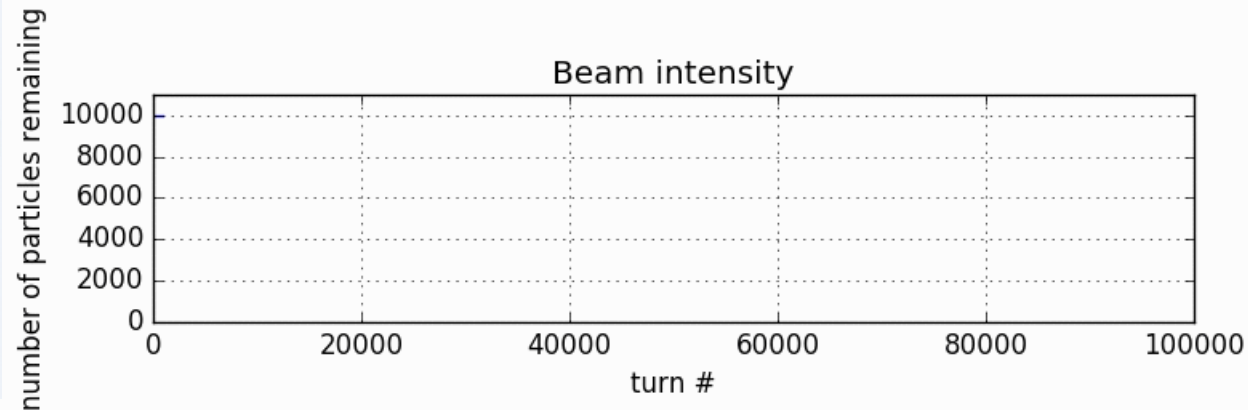
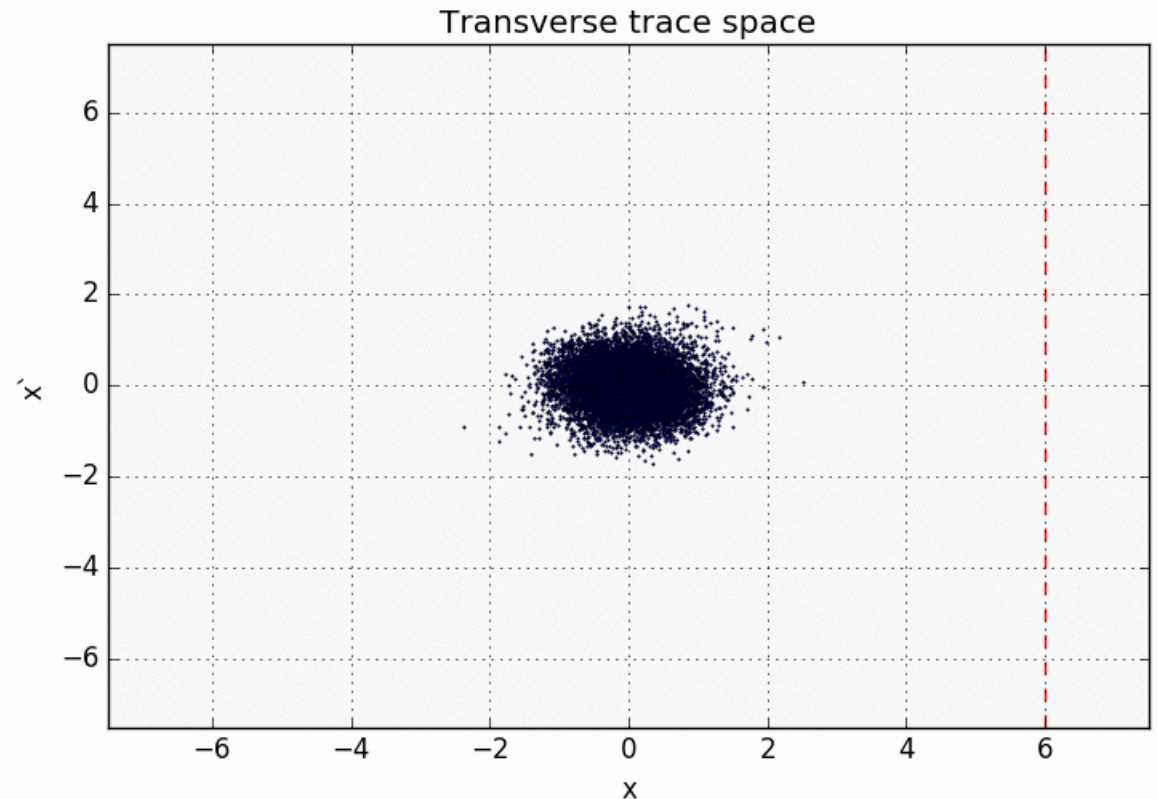
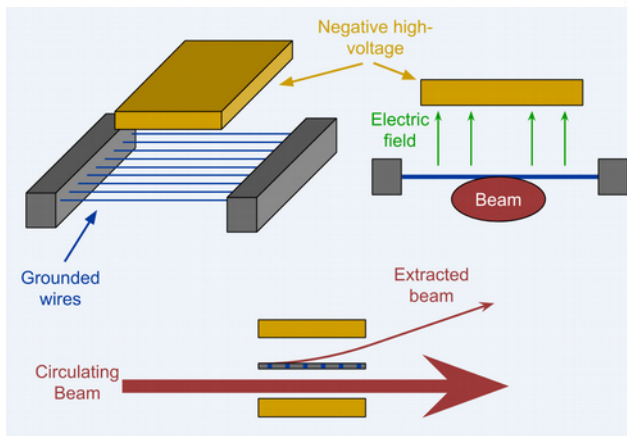
Effect of Non-Linear Fields on Beam

Non-linear fields interact differently with particles on the outside of the ellipse than those toward the core. Thus the fringe particles will rotate at a different rate compared to the core, causing “filamentation”. The beam is no longer elliptical, and requires higher moments to describe. Profiles no longer fit Gaussian distributions as well.



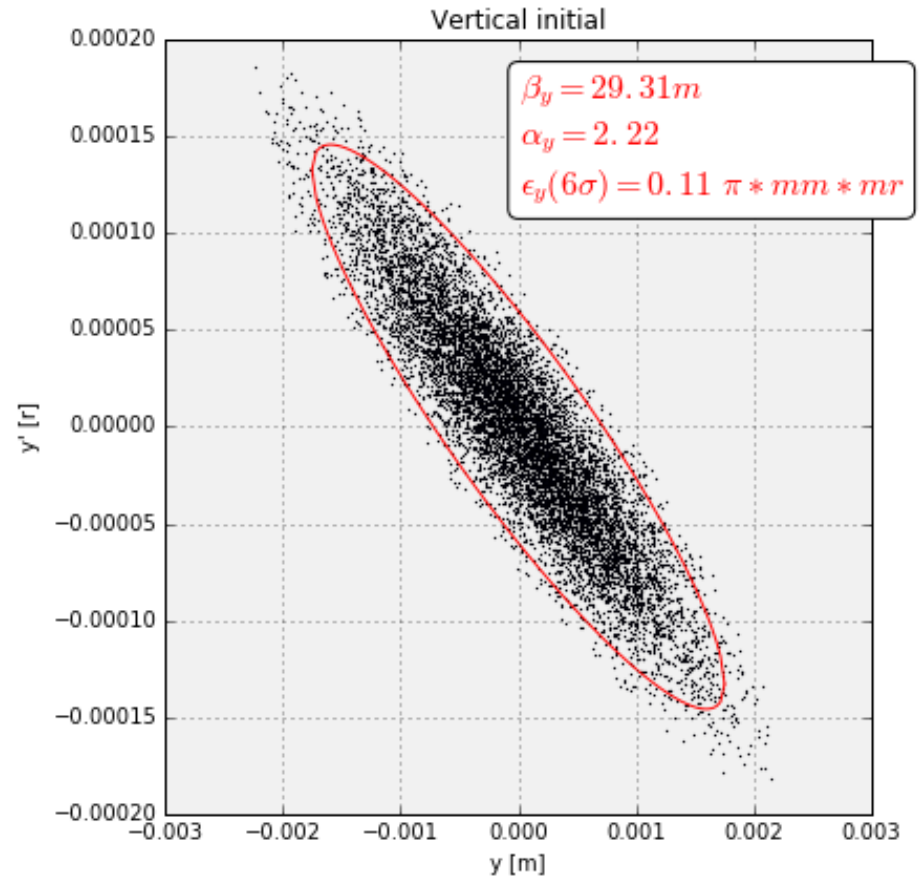
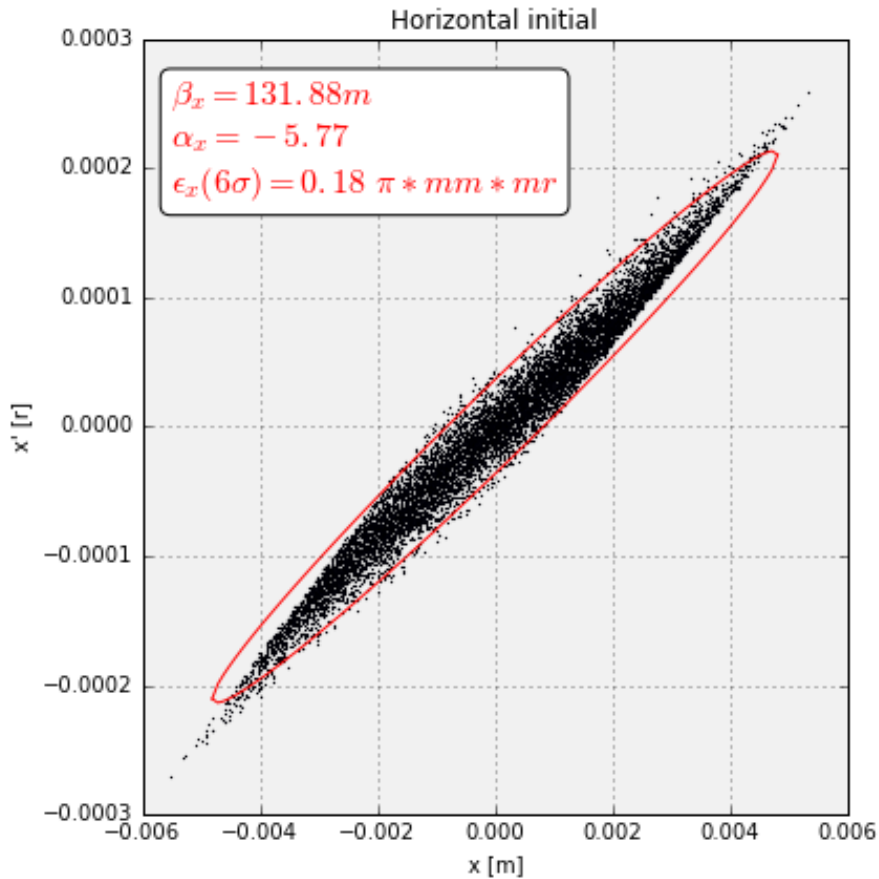
Non-Linear Resonant Extraction

In the Fermilab Switchyard, we take advantage of this nonlinear filamentation, as well as resonance conditions in the betatron oscillations in the Main Injector, to slowly “spill” the beam out to the experiments. The extracted beam is non-elliptical!



Resonant-Extracted Beam

Below is the accumulated phase space distribution of simulated resonant-extraction beam out of the Fermilab Main Injector. Since we're spilling the beam out in the horizontal plane, the total accumulated distribution is non-elliptical only in that plane.



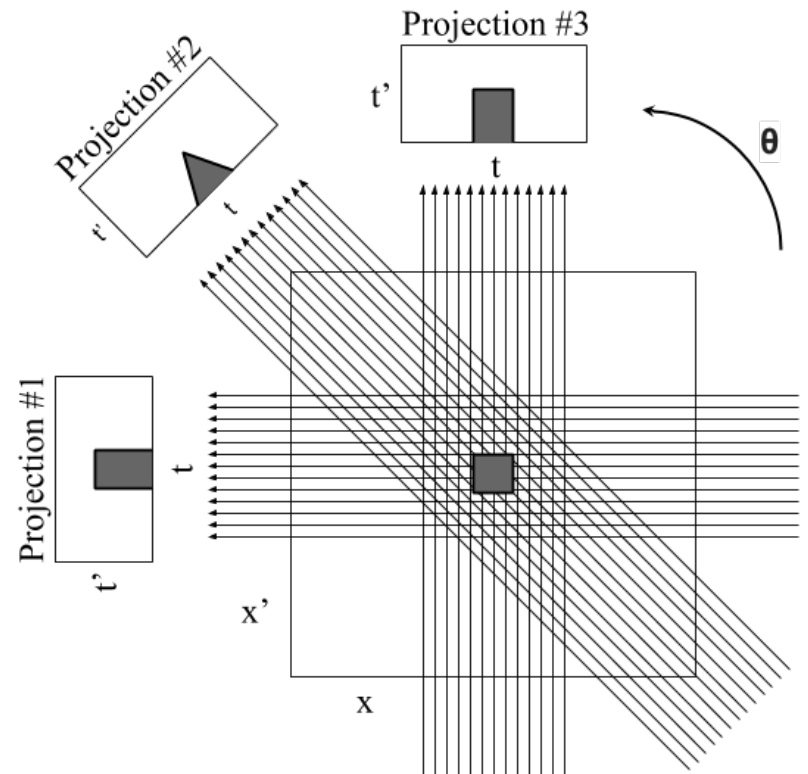
Computed Tomography

Previous methods rely only on second moment propagation, thus assuming elliptical beam. We need a more nuanced method to measure the beam properties that doesn't assume a simple ellipse. Computed tomography reconstructs the non-elliptical phase space distribution from “projections” at different “viewing angles”. Note that since our profile monitors have limited resolution, we are interested in a *discrete* reconstruction of phase space.

Each projection is described by the below equation, known as a “Radon Transform”.

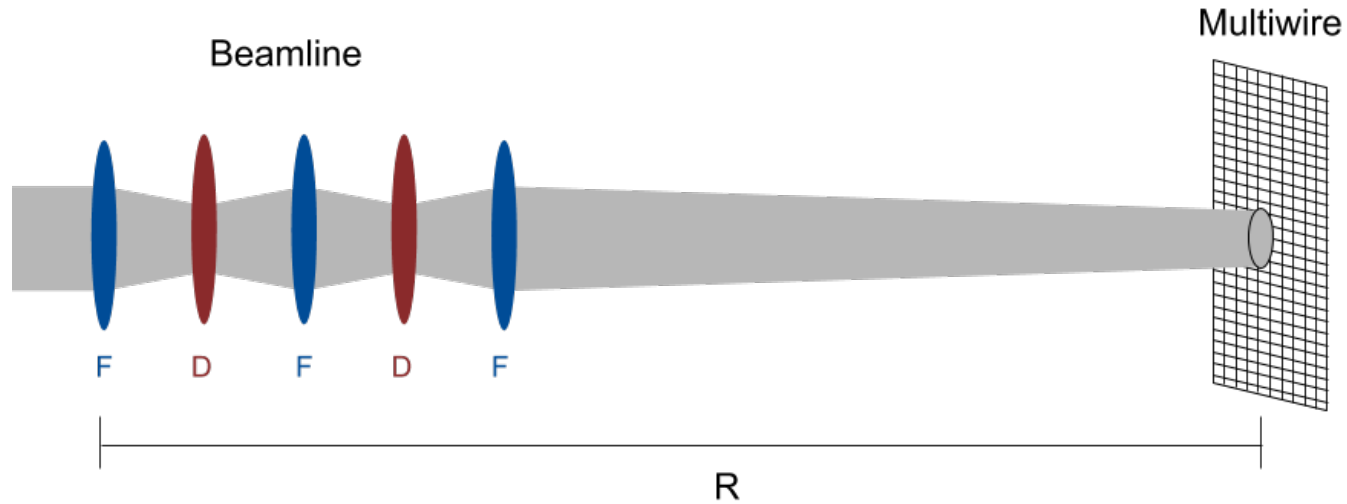
$$P(t, \theta) = \iint dx dy f(x, y) \delta(x \cos \theta + y \sin \theta - t)$$

Countless standard methods exist for reconstructing the original (n)-dimensional image from several (n-1)-dimensional projections, i.e. a reverse Radon Transform. These methods have been studied and developed primarily by mathematicians and the medical imaging industry (“CT” scan is computed tomography).



Computed Tomography and Beam Profiles

Before we can make use of any inverse Radon Transform algorithms, we must make an analogy between beam profiles and projections of a general object.



Projection (beam profile):

$$\begin{pmatrix} x \\ x' \end{pmatrix} = R \begin{pmatrix} x_0 \\ x'_0 \end{pmatrix}$$

$$P(x_0, \theta) = \iint dx dx' f(x, x') \delta(m_{11}x + m_{12}x' - x_0)$$

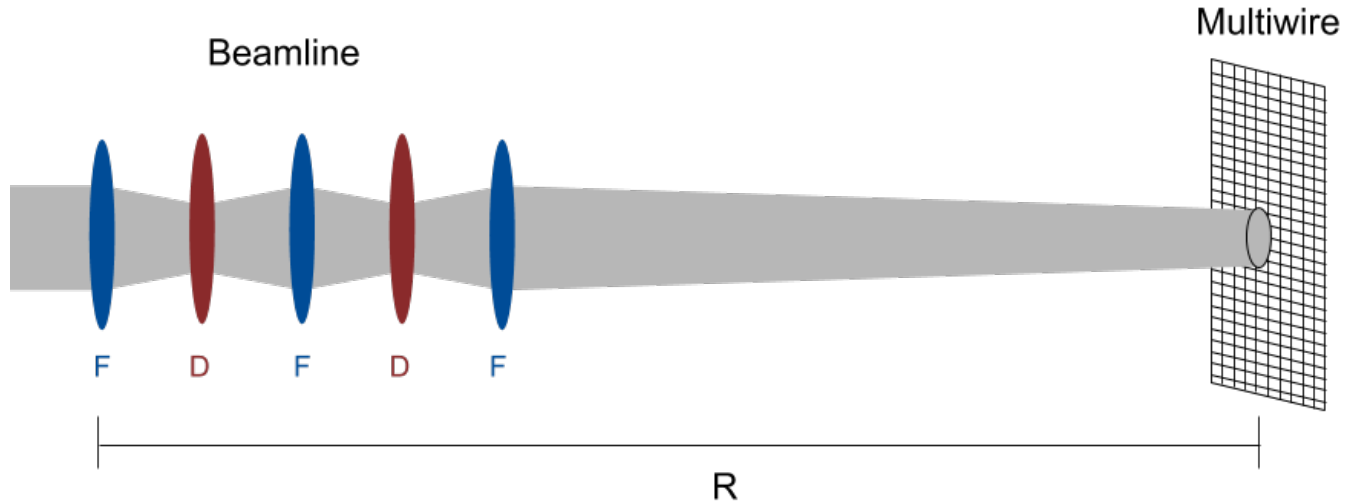
$$R = \begin{pmatrix} m_{11} & m_{12} \\ m_{21} & m_{22} \end{pmatrix}$$

Compare to general projection (Radon Transform):

$$P(t, \theta) = \iint dx dy f(x, y) \delta(x \cos \theta + y \sin \theta - t)$$

Computed Tomography: Beam Profile Scaling

Now we can use standard Computed Tomography algorithms if we scale each profile horizontally and vertically, and use a viewing angle for each profile that depends on the linear optics transfer matrix.



$$s = \sqrt{m_{11}^2 + m_{22}^2}$$

$$\cos\theta = \frac{m_{11}}{s}$$

$$\sin\theta = \frac{m_{12}}{s}$$

$$\theta = \tan^{-1}\left(\frac{m_{12}}{m_{11}}\right)$$

Modified projection (beam profile):

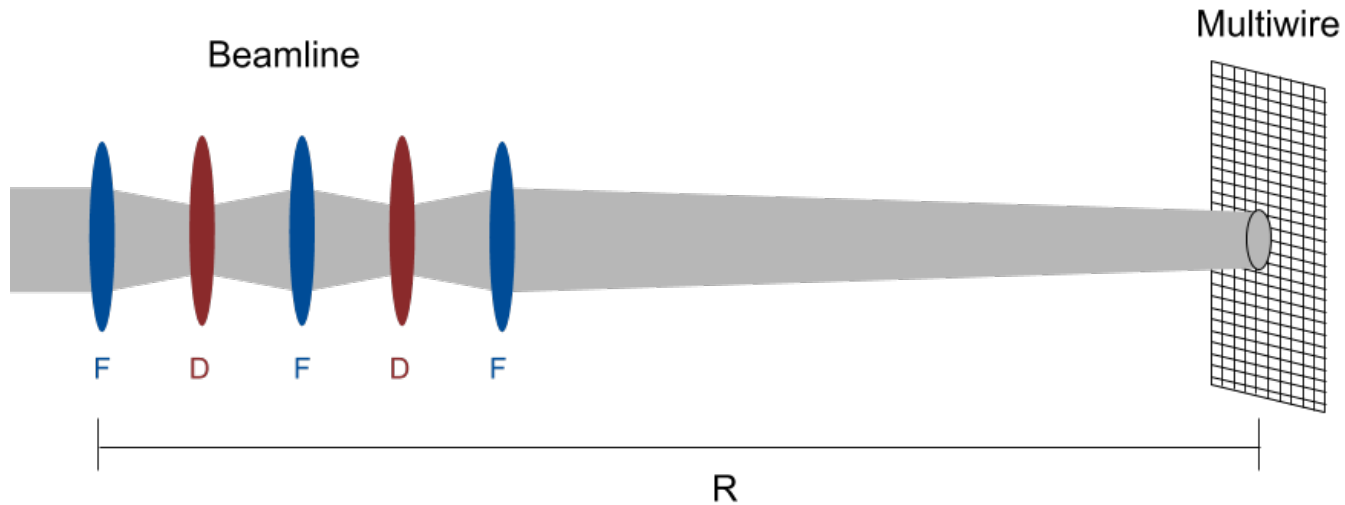
$$P(x_0, \theta) = \iint dx dx' f(x, x') \delta\left(s\left[m_{11}x + m_{12}x' - \frac{x_0}{s}\right]\right)$$

Compare to general projection (Radon Transform):

$$P(t, \theta) = \iint dx dy f(x, y) \delta(x \cos\theta + y \sin\theta - t)$$

Computed Tomography: Beam Profile Scaling

Now we can use standard Computed Tomography algorithms if we scale each profile horizontally and vertically, and use a viewing angle for each profile that depends on the linear optics transfer matrix.



To summarize:

- Vary R matrix between multiwire and point at which we want to reconstruct beam phase space (i.e. scan quadrupoles).
- Take beam profile for each quadrupole setting.
- Scale beam profiles vertically by s and horizontally by $1/s$.
- Apply FBP reconstruction algorithm on scaled profiles, integrating over phase space orientation angle θ .
 - **Note that θ is *not* the betatron phase, and is independent of the beam.

Simultaneous Algebraic Reconstruction Technique

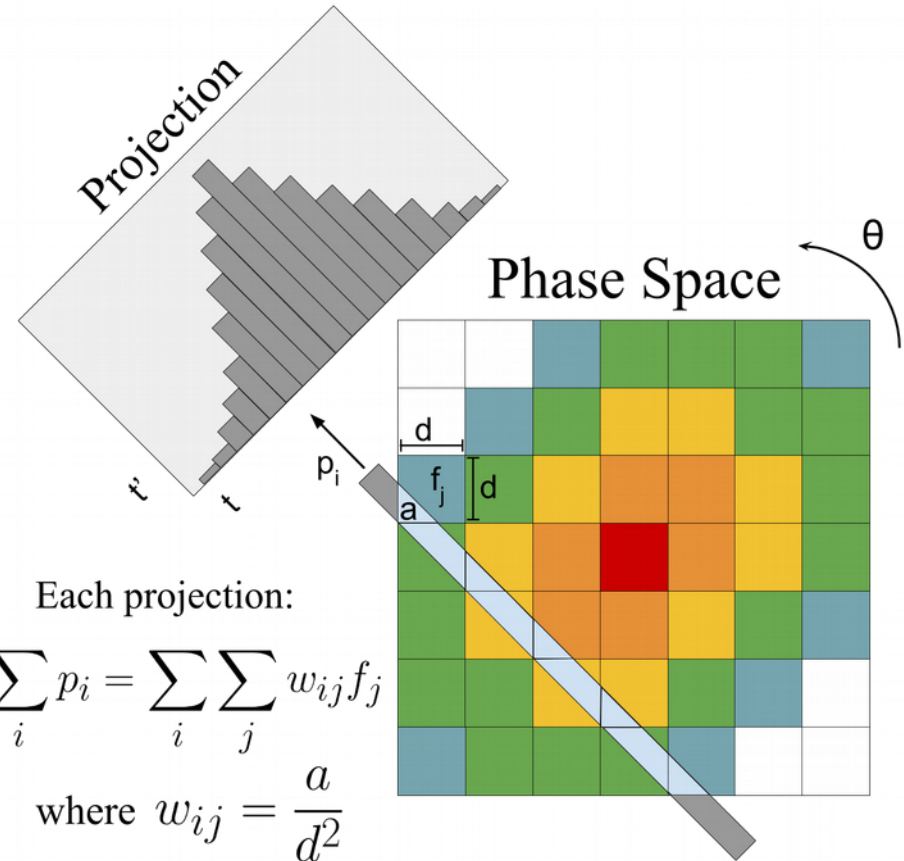
If the original image to be reconstructed is overlain with a grid, or represented as an array of pixels, we can write the following linear system of equations that describe each one-dimensional projection. For N pixels in the original image:

$$\sum_{j=1}^N w_{ij} f_j = p_i$$

The matrix elements w_{ij} represent the fractional area of a pixel subtended by the j^{th} imaging ray. Thus each profile p_i is the sum of the fractional area subtended by all imaging rays, weighted by the value of the original image's pixel f_j .

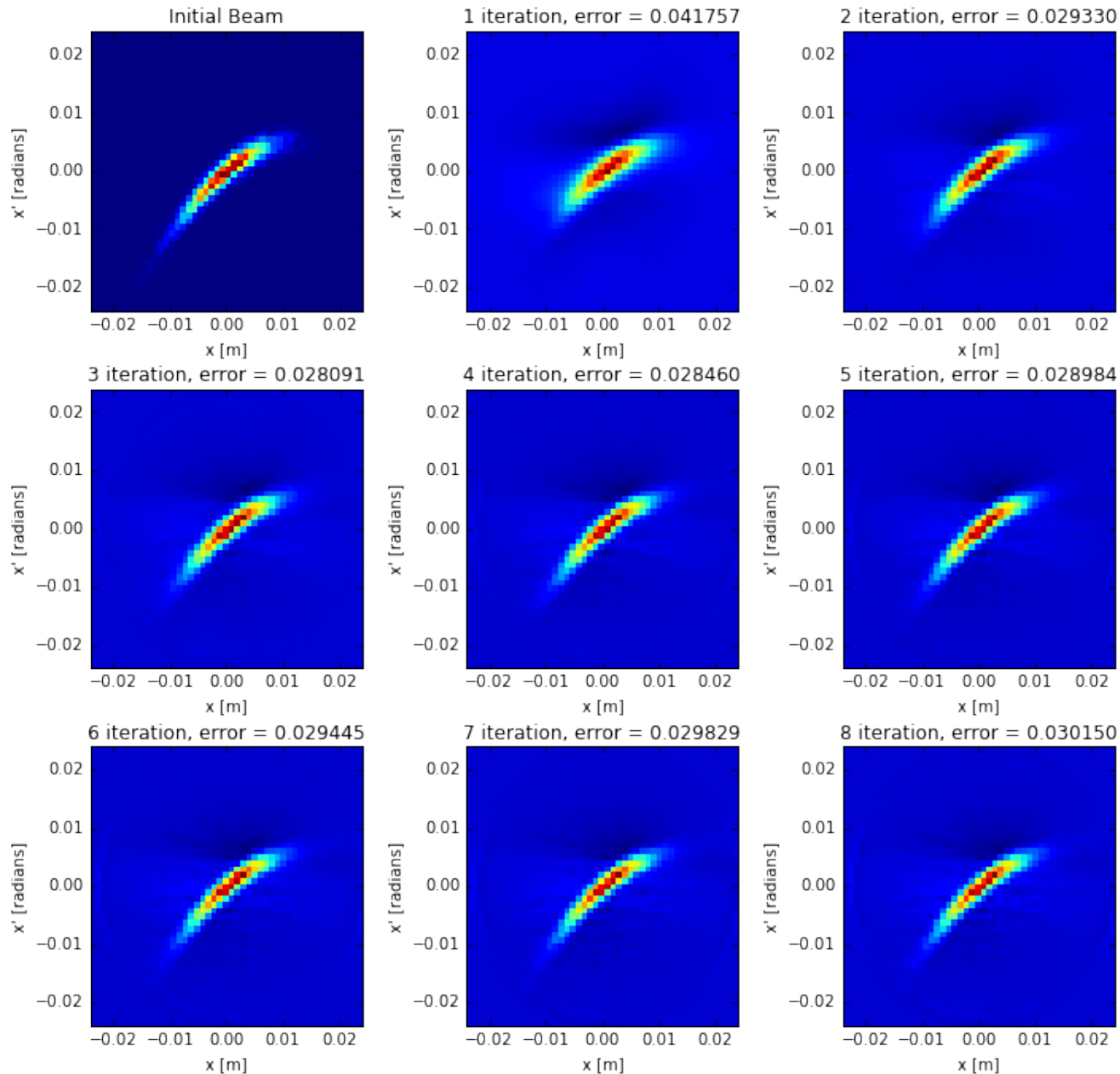
Inverting this system and solving for the values of every pixel f_j reconstructs the original image discretely, and is the purpose of SART.

For N pixels in the original image:



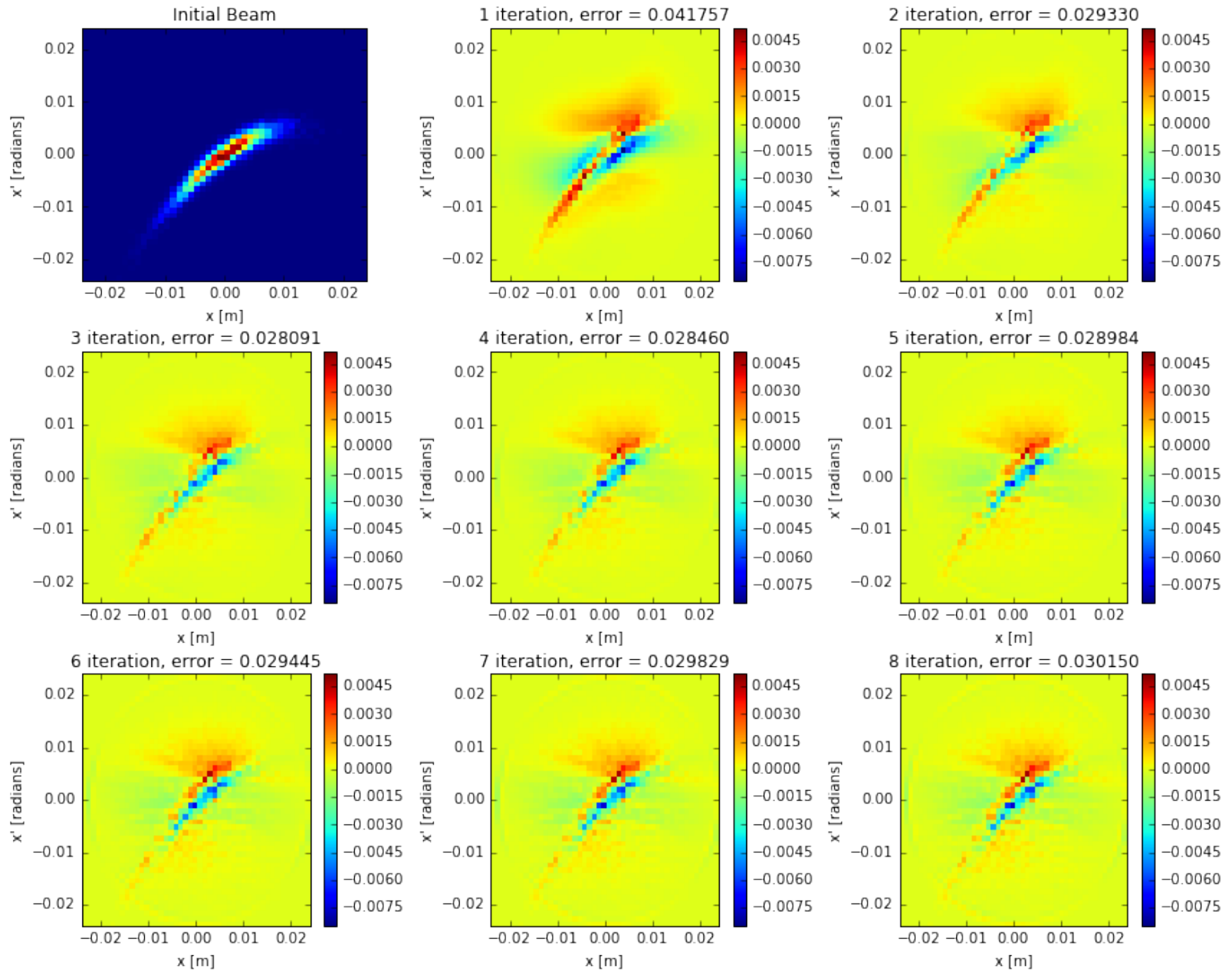
Source: A. C. Kak and Malcolm Slaney, *Principles of Computerized Tomographic Imaging*, IEEE Press, 1988.

SART reconstructions, relax = 0.1



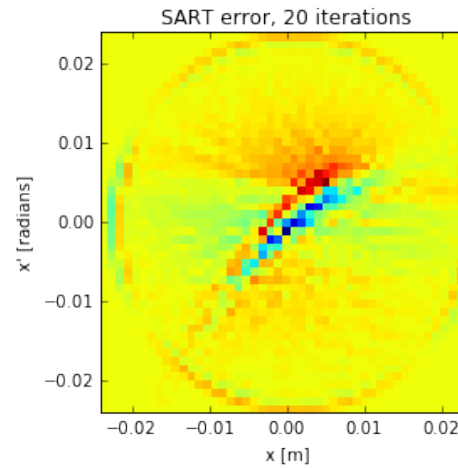
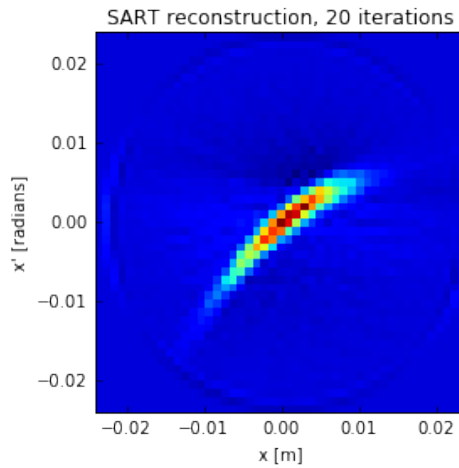
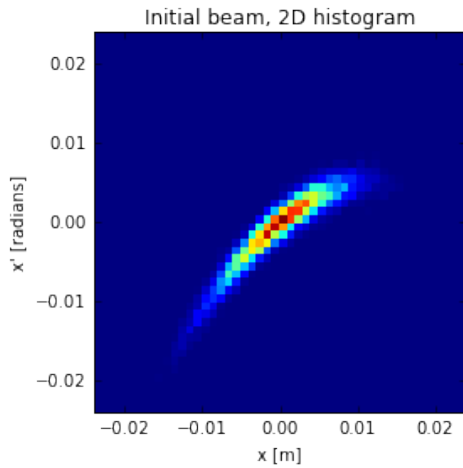
This simulated reconstruction starts by generating a random, non-Gaussian beam phase space distribution. Then it passes each particle through a strong-focusing beamline and collects the simulated multiwire profile at the end. A new profile is collected for each setting of the quadrupoles' gradient, thus varying the viewing angle. Then SART is applied

SART errors, relax = 0.1

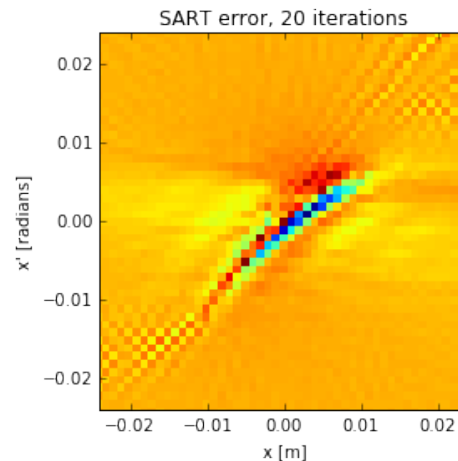
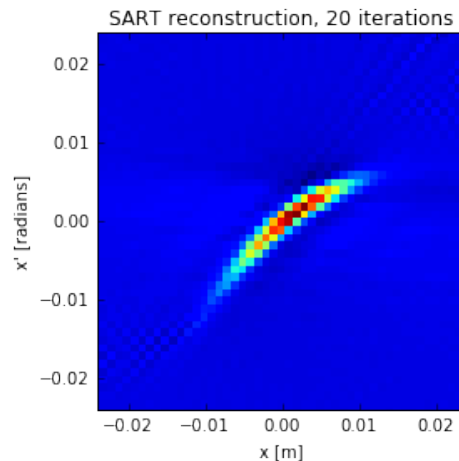
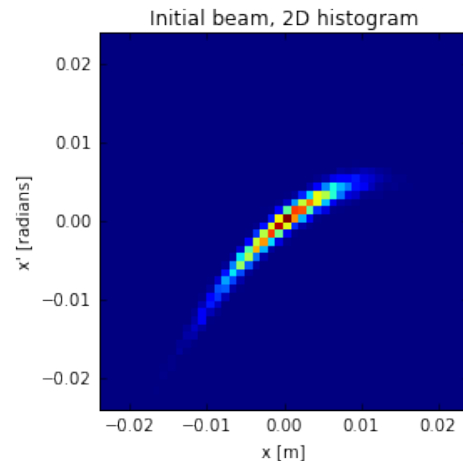


SART with many iterations

Tail reconstruction appears improved for larger iteration values, though artifacts begin to dominate. Over-iteration seems to improve tail reconstruction somewhat, but at the cost of “salt and pepper” noise, as well as phantom ring surrounding the beam. This ring is not present for a bigger multiwire, so presumably the ring artifact is due to beam clipping on the multiwire aperture.



**4.8mm-wide
multiwire**



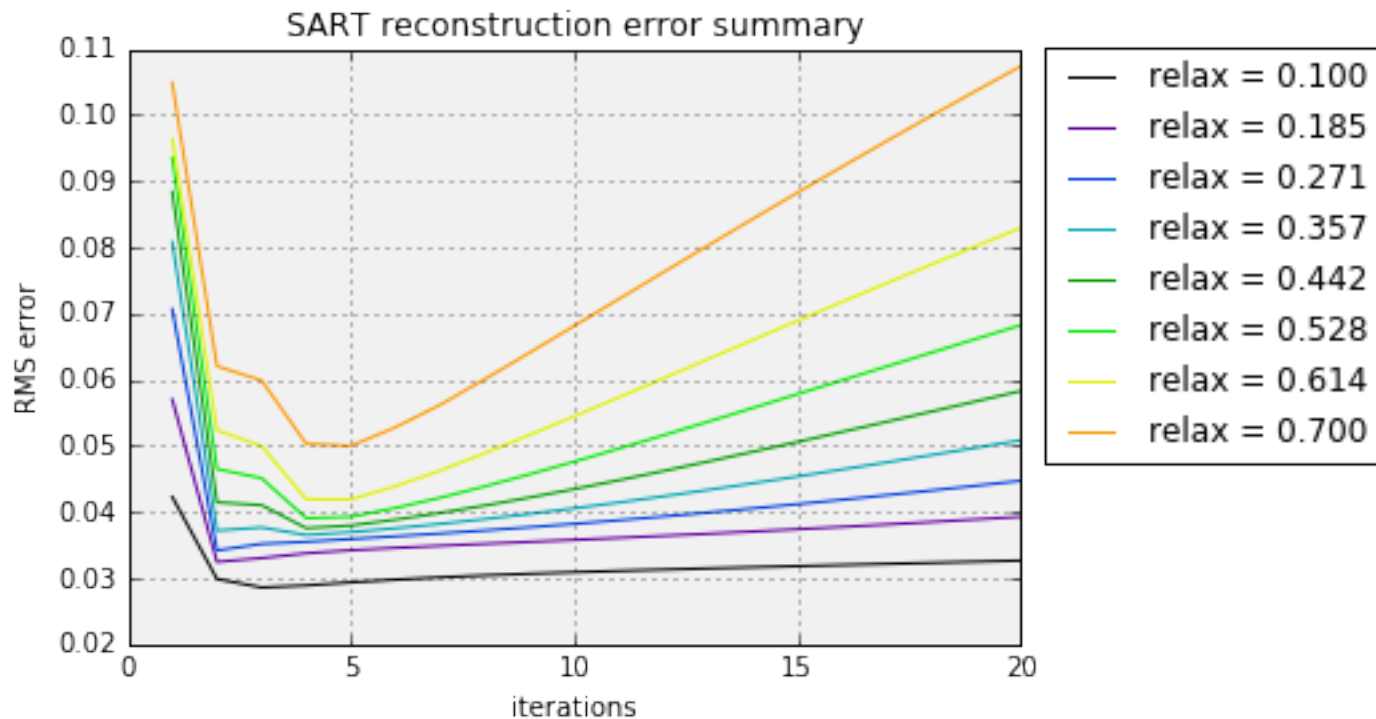
**19.2cm-wide
multiwire**

Optimization of SART

Now we vary the “relaxation” parameter and investigate the quality of reconstruction as a function of successive iterations. The RMS error is used as the figure of merit to determine reconstruction quality.

The resulting plot helps determine the combination of relaxation parameter and number of iterations that produce the best reconstruction, i.e. that which is most faithful of the original distribution.

It is apparent that increased iterations and relaxation value contribute to increased artifacts, presumably due to the propagation of noise/artifacts from previous iterations. A balance between iterations and relaxation provides best overall result (i.e. lowest RMS error)



Conclusion

We will soon be taking real beam data to reconstruct using SART Computed Tomography. This reconstruction will allow us to compute an effective Courant-Snyder ellipse that can serve as the initial condition into our beamline optics models. The hope is that this will greatly improve our models' predictive power and allow us to re-tune to improve efficiency.

Traditional methods of measuring the beam ellipse have proven error-prone with non-elliptical beam. Because of our resonant extraction process, as well as non-linearities in the magnets of our very long beamlines, we cannot assume a phase space ellipse *a priori*. Thus, Computed Tomography will let us image our beam phase space more directly.

References and Resources

- Edwards, D. A. and Syphers, M. J. (1993) Frontmatter, in An Introduction to the Physics of High Energy Accelerators, Wiley-VCH Verlag GmbH, Weinheim, Germany. doi: 10.1002/9783527617272.fmatte; <http://onlinelibrary.wiley.com/doi/10.1002/9783527617272.fmatter/summary>
- Fermilab Accelerator Division Operations Department. Concepts Rookie Book (Beams Document 4444). http://operations.fnal.gov/rookie_books/concepts.pdf
- Watts, Adam. "Measurement of Elliptical Beam Emittance in the Transverse Plane". <http://beamdocs.fnal.gov/AD-public/DocDB/ShowDocument?docid=5323>
- United States Particle Accelerator School: uspas.fnal.gov
- D. Stratakis, Ph.D. Dissertation, "Tomographic Measurement of the Phase Space Distribution of a Space-Charge-Dominated Beam", University of Maryland, 2008; http://www.umer.umd.edu/publications/Theses/Stratakis_Dissertation_Final_v3.pdf
- Watts, Adam et. al., "Computed Tomography of Transverse Phase Space". 2016 North American Particle Accelerator Conference (NAPAC'16), TUPOA36; <http://vrws.de/napac2016/papers/tupoa36.pdf>
- Fermilab Accelerator Division External Beamlines Department: extbeams.fnal.gov
- Python Anaconda: <https://www.continuum.io/downloads>
- Python "scikit-image" library: <http://scikit-image.org/>
- Christofilos, N. C. (1950). "Focusing System for Ions and Electrons". US Patent No. 2,736,799.
- Courant, E. D.; Snyder, H. S. (Jan 1958). "Theory of the alternating-gradient synchrotron" (PDF). Annals of Physics. 3 (1): 1–48. Bibcode:2000AnPhy.281..360C. doi:10.1006/aphy.2000.6012.
- A. C. Kak and Malcolm Slaney, Principles of Computerized Tomographic Imaging, IEEE Press, 1988.
- Fermilab Job Postings: <https://jobs-us.technomedia.com/fermilab/>

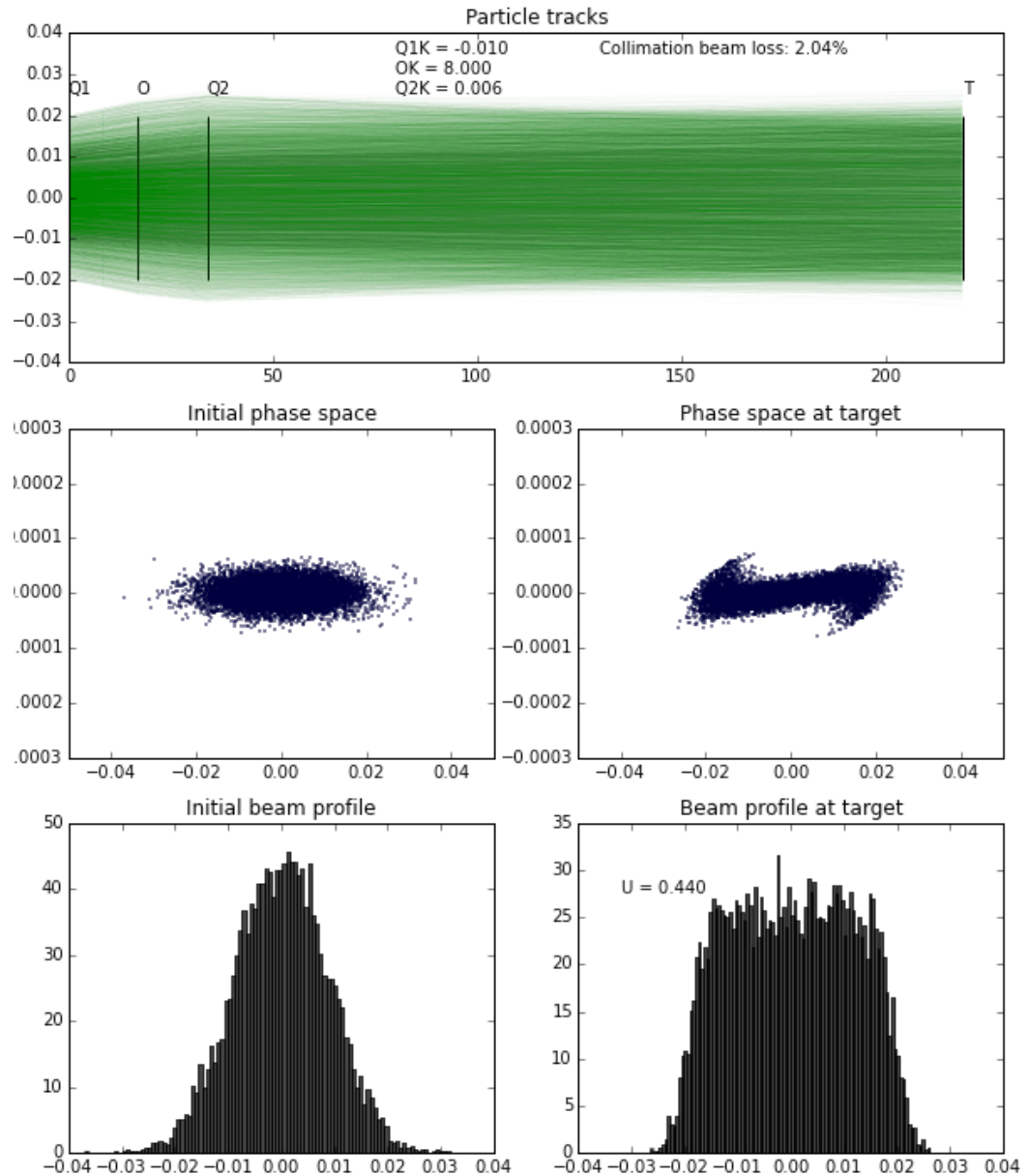
Thank you!

awatts@fnal.gov

Backup Slides

A Use for Non-Linear Magnets

An octupole in a beamline can, if placed appropriately, create a more uniform distribution on an experimental target. For example, if an experiment needs very uniform heating of a cryogenic target, one octupole (or two sextupoles) per plane can achieve the desired profile.



An Added Complication: Chromatic Effects

The bend radius of a dipole and the focal length of a quadrupole depend on the particle's momentum (because of the rigidity term “B-rho”). We typically compare momentum offsets to some “reference” momentum, and characterize the shift in position and focal length by the fractional deviation in momentum as compared to the reference particle. Position offset due to momentum offset is known as “Dispersion”, and focal length offset due to momentum offset is called “Chromatic Aberration”. This is the same chromatic aberration found in traditional optics, where light of different colors is focused differently by the same lens.

$$\Delta\theta = \frac{BL}{(B\rho)}$$

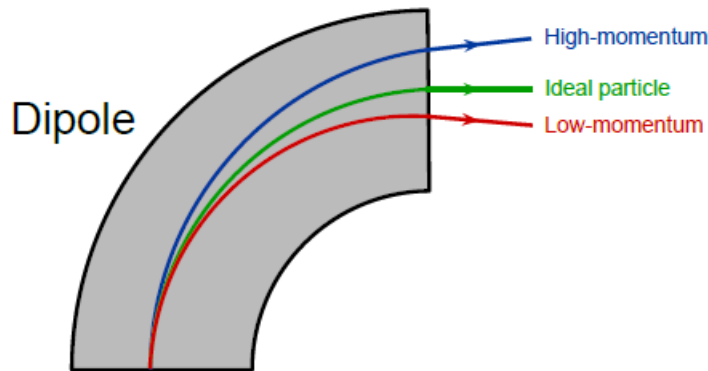


Figure 2.6: Dipole magnet dispersion.

$$\Delta x \propto D_1 \frac{\Delta p}{p} + D_2 \left(\frac{\Delta p}{p}\right)^2 + \dots$$

$$\frac{1}{f} = \frac{B'L}{(B\rho)}$$

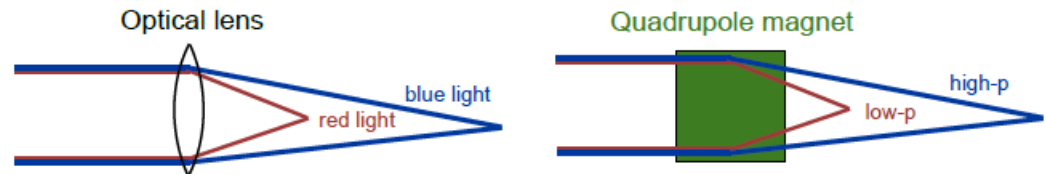


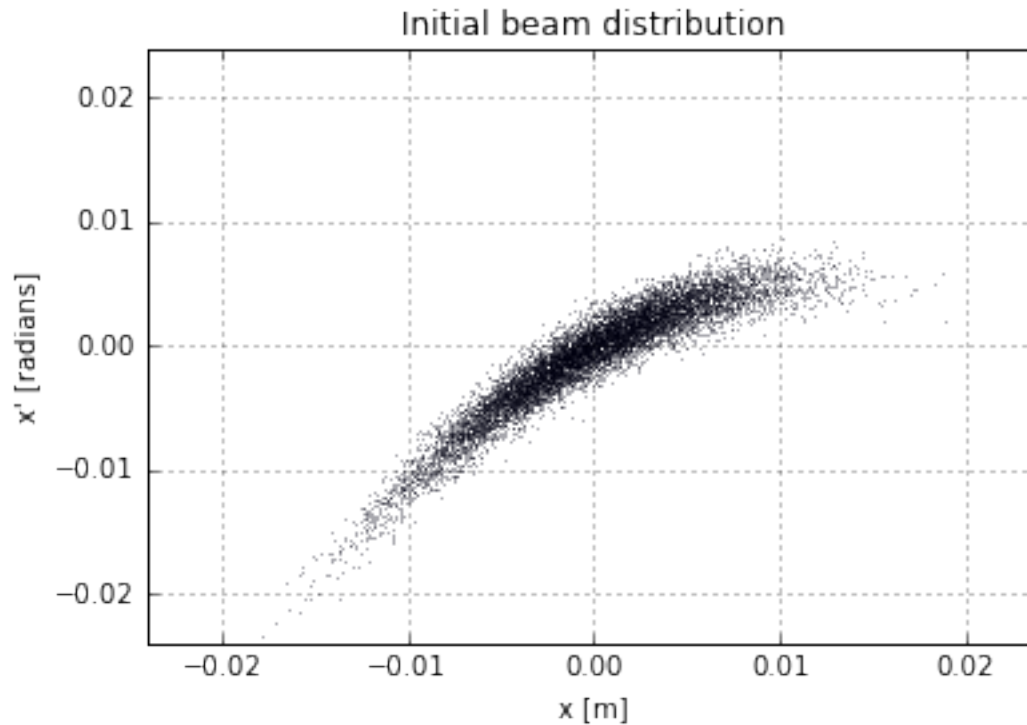
Figure 2.11: Chromatic aberration in optics and beam physics.

$$\Delta f \propto \xi_1 \frac{\Delta p}{p} + \xi_2 \left(\frac{\Delta p}{p}\right)^2 + \dots$$

Beam simulation (Python code)

Generate initial random beam distribution with asymmetry and tails:

```
sigmax = 0.005  
sigmaxp = sigmax/4  
x0 = np.random.normal(0, sigmax, 10000)  
xp0 = -30*x0**2 + 0.8*x0 + np.random.normal(0, sigmaxp, 10000)
```



Beam simulation (Python code)

Pass each particle through linear optics, i.e. simple FODO channel:

```
L = 1 # drift length [m]
O = np.array([[1,L],[0,1]])
F = np.array([
    [np.cos(k**0.5), (k**-0.5)*np.sin(k**0.5)],
    [-(k**0.5)*np.sin(k**0.5), np.cos(k**0.5)]
])
D = np.array([
    [np.cosh(k**0.5), (k**-0.5)*np.sinh(k**0.5)],
    [-(k**0.5)*np.sinh(k**0.5), np.cosh(k**0.5)]
])

R = np.linalg.multi_dot([O,D,O,F,O,D,O,F,O,D,O,F])

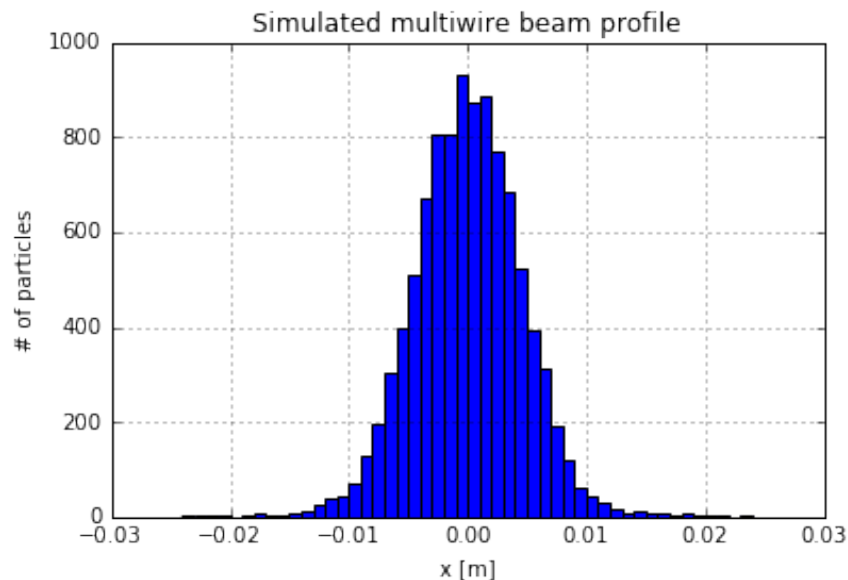
xnew = R[0][0]*x + R[0][1]*xp
xpnew = R[1][0]*x + R[1][1]*xp
```

Beam simulation (Python code)

Simulate a multiwire profile by using a fixed-width fixed-bin histogram on all “x” values:

```
num_wires = 48
wire_pitch = 0.001
low_x_lim = -(num_wires/2)*wire_pitch
high_x_lim = (num_wires/2)*wire_pitch
binBoundaries = np.linspace(low_x_lim,high_x_lim,num_wires+1)

hystarray = plt.hist(xnew,bins=binBoundaries)[0]
```



Beam simulation (Python code)

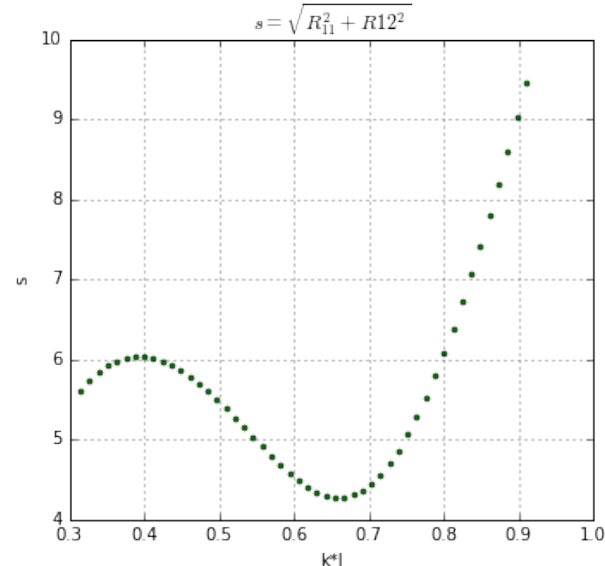
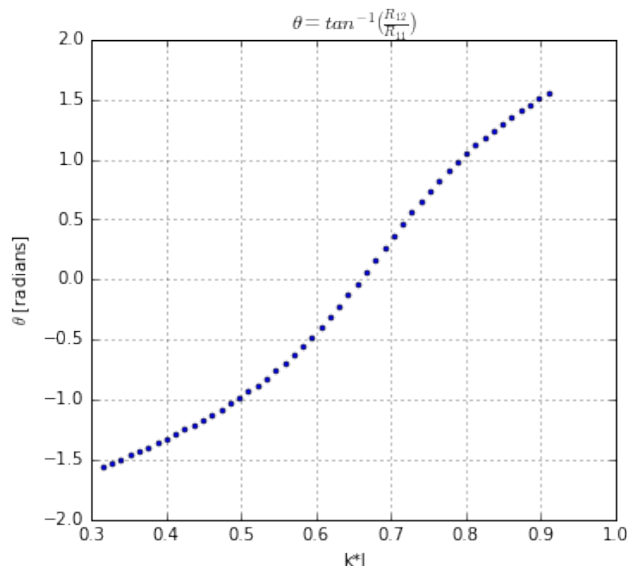
Repeat process for each new beamline tune by varying the k values of all the quadrupoles. Thus we collect beam profiles for each new phase space orientation angle θ . We want to have “enough” projections at angles spanning as close to 180 degrees as possible.

```
k_array = np.linspace(0.315,0.91,50)
```

After each profile is taken, calculate the scaling factor and orientation angle for that tune.

```
theta = np.arctan(R[0][1]/R[0][0])  
s = np.sqrt(R[0][0]**2+R[0][1]**2)
```

Choice of the k values in the array depends on how many projections we want (i.e. “a lot”), and how wide a range of θ we can achieve.



Beam simulation (Python code)

Collect all the profiles into a single structure known as a *sinogram* that summarizes how the beam profile changed as a function of orientation angle. Then scale each profile vertically by s and horizontally by $1/s$.

Scaled and un-scaled sinograms are shown below for comparison. Note that there is clipping of the beam tails due to the finite size of the multiwire.

